Inorganic Chemistry

Article

pubs.acs.org/IC

Modeling Tyrosinase and Catecholase Activity Using New *m*-Xylyl-Based Ligands with Bidentate Alkylamine Terminal Coordination

Sukanta Mandal,[†] Jhumpa Mukherjee,[†] Francesc Lloret,[‡] and Rabindranath Mukherjee*[,†,§]

[†]Department of Chemistry, Indian Institute of Technology Kanpur, Kanpur 208 016, India

[‡]Departament de Química Inorgànica/Instituto de Ciencia Molecular (ICMOL), Universitat de València, Polígono de la Coma, s/n, 46980 Paterna (València), Spain

Supporting Information

ABSTRACT: Chemical model systems possessing the reactivity aspects of both tyrosinase and catechol oxidase are presented. Using two *m*-xylyl-based ligands providing bidentate alkylamine terminal coordination, 1,3-bis[(*N*,*N*-dimethylaminoethyl)aminomethyl]benzene ($L^{H,H}$) and 1,3-bis[(*N*,*N*,*N*′-trimethylaminoethyl)aminomethyl]benzene ($L^{Me,Me}$), four new dicopper(I) complexes, $[Cu^{I}_2(L^{H,H})(MeCN)_4][ClO_4]_2$ (**1**), $[Cu^{I}_2(L^{H,H})(PPh_3)_2(MeCN)_2][ClO_4]_2$ (**2**), $[Cu^{I}_2(L^{Me,Me})(MeCN)_2][ClO_4]_2$ (**3**), and $[Cu^{I}_2(L^{Me,Me})(PPh_3)_2][ClO_4]_2$ (**4**), have been synthesized and characterized. Complex **2** has been structurally characterized. Reaction of the dicopper(I) complex $\mathbf{3}^{2+}$ with dioxygen at 183 K generates putative bis(μ−oxo)dicopper(III) intermediate (absorption spectroscopy). Oxygenation of **1** and **3** brings about *m*-xylyl-ring hydroxylation (monooxygenase-like activity), with a noticeable color change from pale-yellow to dark green. The presence of phenoxo- and hydroxo-bridges in the end products $[Cu^{II}_2(L^{H,H}{-}O)(OH)(MeCN)_2][ClO_4]_2$ (**5**) and $[Cu^{II}_2(L^{Me,Me}{-}O)(OH)(OClO_3)][ClO_4]\cdot MeCN$(**6**) has been authenticated by structural characterization. Oxygenation of **3** afforded not only the green complex **6** isolation but also a blue complex $[Cu^{II}_2(L^{Me,Me})(OH)_2][ClO_4]_2$ (**7**). Variable temperature magnetic susceptibility measurements on **5** and **6** establish that the Cu^{II} centers are strongly antiferromagnetically coupled [singlet−triplet energy gap (J) = −528 cm^{-1} (**5**) and −505 cm^{-1} (**6**)]. The abilities of phenoxo- and hydroxo-bridged dicopper(II) complexes **5** and **6**, the previously reported complex $[Cu^{II}_2(L^{1}{-}O)(OH)(OClO_3)_2]\cdot 1.5H_2O$ (**8**) (L^1−OH = 1,3-bis[(2-dimethylaminoethyl)iminomethyl]phenol), and $[Cu^{II}_2(L^{2}{-}O)(OH)(OClO_3)][ClO_4]$ (**9**) (L^2−OH = 1,3-[(2-dimethylaminoethyl)iminomethyl][(*N*,*N*,*N*′-trimethyl)aminoethyl]-4-methylphenol) have been examined to catalyze the oxidation of catechol to quinone (catecholase activity of tyrosinase and catechol oxidase-like activity) by employing the model substrate 3,5-di-*tert*-butylcatechol. Saturation kinetic studies have been performed on these systems to arrive at the following reactivity order [k_{cat}/K_M (catalytic efficiency) × 10^{-3} (M^{-1} h^{-1})]: 470 (**6**) > 367 (**5**) > 128 (**9**) > 90 (**8**).

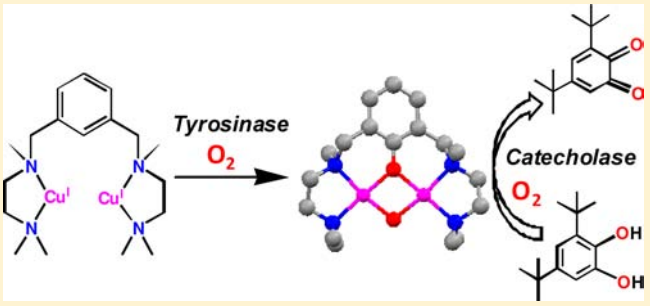

INTRODUCTION

Despite the structural similarity (three histidines bound to each copper center in bimetallic active sites), the three Type 3 copper proteins exhibit different reactivity.[1,2] Hemocyanin is a dioxygen carrier. Tyrosinase acts as a monooxygenase, binding of O_2 is followed by activation to further process it, and catechol oxidase acts as a simple oxidase. Tyrosinase is a particularly interesting enzyme to catalyze the initial step in the formation of the pigment melanin from tyrosine. It catalyzes the aerial oxidation of monophenols like tyrosine to *o*-diphenols (*ortho*-hydroxylation of phenols, monophenolase activity) and the oxidation of *o*-diphenols (catechols) like DOPA to *o*-quinones (catecholase activity).[1−3] The ubiquitous plant enzyme catechol oxidase, in contrast to tyrosinase, catalyzes exclusively the oxidation of catechols to the corresponding *o*-quinones by molecular oxygen, without acting on monophenols.[1b,2,4] Extensive work has been done to unravel the reaction mechanism of tyrosinase.[5−7] The generally accepted mechanism proposes that a (μ−η^2:η^2-peroxo)-dicopper(II) ***P*** species is responsible for the hydroxylation step via an electrophilic attack on the aromatic ring. The observation that the ***P*** core can exist in equilibrium with its bis(μ-oxo)dicopper(III) ***O*** isomer,[8] is suggestive of the proposal that the ***O*** species may also be responsible for the arene hydroxylation step. In fact, evidence has been provided that the ***O*** species can effect intramolecular arene-ring hydroxylation,[9] as well as *ortho*-hydroxylation of externally added phenolate to the corresponding catechol.[10−12] Notably, for the *m*-xylyl-based system, analysis of the ligand after thermal decay of the ***O*** intermediate did not show any evidence for intramolecular xylyl-ring hydroxylation.[11]A recent study has demonstrated that an end-on *trans*-peroxide dicopper(II) species, supported by the *m*-xylyl-based system, also exhibits

Received: June 28, 2012
Published: November 29, 2012

monooxygenase activity.[13] Although not explicitly stated, it is implied that this system did not show any evidence for intramolecular xylyl-ring hydroxylation. Thus, the understanding of the reaction of molecular O_2 with Cu^I complexes, supported by various terminal ligands, and the isolation and structural characterization of side-on-peroxo-dicopper(II) or bis-oxo-dicopper(III) complexes is one of the key issues.[14−18]

As a part of our own interest in the investigations of the reactions of Cu^I complexes with molecular oxygen,[19−21] to demonstrate (i) ring hydroxylation reactions[22−28] using *m*-xylyl-based ligands with two nitrogen donor terminal sites and (ii) the formation (low-temperature absorption spectroscopy) and reactivity aspects of the ***O*** intermediate,[29] we directed our attention to a group of *m*-xylyl-based ligands, providing terminal bidentate alkylamine coordination (Figure 1). Herein,

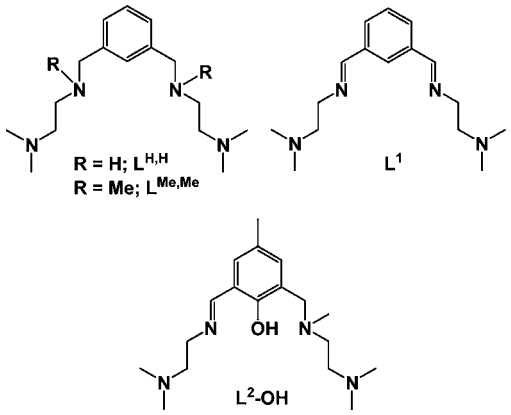

Figure 1. The ligands chosen in this work.

we describe the syntheses and characterization of dinuclear copper(I) complexes, $[Cu^I_2(L^{H,H})(MeCN)_4][ClO_4]_2$ (**1**), $[Cu^I_2(L^{H,H})(PPh_3)_2(MeCN)_2][ClO_4]_2$ (**2**), $[Cu^I_2(L^{Me,Me})(MeCN)_2][ClO_4]_2$ (**3**), and $[Cu^I_2(L^{Me,Me})(PPh_3)_2][ClO_4]_2$ (**4**), and copper(II) complexes, $[Cu^{II}_2(L^{H,H}-O)(OH)(MeCN)_2][ClO_4]_2$ (**5**), $[Cu^{II}_2(L^{Me,Me}-O)(OH)(OClO_3)][ClO_4]\cdot MeCN$ (**6**), and $[Cu^{II}_2(L^{Me,Me})(OH)_2][ClO_4]_2$ (**7**). Structural characterizations of **2**, **5**, and **6** have been achieved. Reaction of dicopper(I) complex of $L^{Me,Me}$ $\mathbf{3}^{2+}$ with dioxygen at 183 K generates putative ***O*** intermediate (absorption spectra). Significantly, ***O*** intermediate decays with concomitant intramolecular xylyl-ring hydroxylation (monooxygenase-like activity). Using a *m*-xylyl-based ligand, this is a result observed for the first time. In fact, intramolecular ligand hydroxylation has been observed with both the ligands, $L^{H,H}$ and $L^{Me,Me}$.

The phenoxo- and hydroxo-bridged dicopper(II) complexes **5**, **6**, $[Cu^{II}_2(L^1-O)(OH)(OClO_3)_2]\cdot 1.5H_2O$ (**8**),[28] and $[Cu^{II}_2(L^2-O)(OH)(OClO_3)][ClO_4]$ (**9**)[30,31] have been shown to catalyze the aerobic oxidation of catechol to quinone by employing 3,5-di-*tert*-butylcatechol (3,5-DTBC).[32−43] To throw light on the mechanistic aspects, saturation kinetic studies (excess substrate) have also been done on **5**, **6**, **8**, and **9**. The comparative analysis pinpoints the subtle effect of the nature of the donor atom type on the binding of the substrate at the dicopper(II) site and subsequent catalytic potential to exhibit catechol oxidase-like activity.

EXPERIMENTAL SECTION

Reagents and Materials. All chemicals were obtained from commercial sources and used as received. Solvents were dried as reported previously.[19,28,29] All air-sensitive reactions were performed either in an inert-atmosphere glovebox (MBraun, Germany) under a N_2 atmosphere or by using standard Schlenk- and vacuum-line techniques. $[Cu^I(MeCN)_4][ClO_4]$,[44a] $[Cu^I(MeCN)_4][CF_3SO_3]$,[44b] and $[Cu^I(MeCN)_4][PF_6]$[44c] were prepared following literature reports. The sodium salt of 2,4-di-*tert*-butylphenolate was synthesized following a similar procedure as reported for sodium *p*-chlorophenolate in the literature.[11] Isolation and handling of dicopper(I) complexes were carried out inside the glovebox. The complexes $[Cu^{II}_2(L^1-O)(OH)(OClO_3)_2]\cdot 1.5H_2O$ (**8**)[28] and $[Cu^{II}_2(L^2-O)(OH)(OClO_3)][ClO_4]$ (**9**)[30,31] were prepared following the reported procedures.

Syntheses of Ligands. 1,3-Bis[(*N,N*-dimethylaminoethyl)aminomethyl]benzene ($L^{H,H}$). The synthetic strategy comprises the following two steps.

1,3-Bis[(2-dimethylaminoethyl)iminomethyl]benzene (L^1). This was synthesized from isophthalaldehyde and *N,N*-dimethylethylenediamine as described previously.[28]

1,3-Bis[(*N,N*-dimethylaminoethyl)aminomethyl]benzene ($L^{H,H}$). The ligand L^1 (2.00 g, 7.29 mmol) was dissolved in dry MeOH (15 mL) and heated on a steam bath. To it, excess $NaBH_4$ (1.66 g, 43.92 mmol) was added in small portions. After each addition, the mixture was thoroughly shaken. After cooling, a saturated brine solution (25 mL) was added and the reduced product was extracted with Et_2O (5 × 10 mL). The organic layer was collected and kept with anhydrous K_2CO_3. On evaporation of the solvent, the desired product was obtained as yellow oil. Yield: 1.95 g, 96%. Anal. Calcd (%) for $C_{16}H_{30}N_4\cdot 3H_2O$: C, 57.80; H, 10.91; N, 16.85. Found: C, 57.92; H, 10.35; N, 16.73. ^{1}H NMR (400 MHz, CD_3CN): δ 1.93 (br, 2H, N*H*), 2.16 (12H, *s*, $-N(CH_3)_2$), 2.36 [4H, *t*, J = 6 Hz, $-HNCH_2CH_2N(CH_3)_2$], 2.62 [4H, *t*, J = 6 Hz, $-HNCH_2CH_2N(CH_3)_2$], 3.75 (4H, *s*, *m*-xylyl-CH_2NH-), 7.17−7.38 (4H, *m*, aromatic protons). ^{13}C NMR (400 MHz, CD_3CN): δ 44.82 [$-N(CH_3)_2$], 46.56 [$-HNCH_2CH_2N(CH_3)_2$], 53.47 (*m*-xylyl-CH_2NH-), 59.30 [$-HNCH_2CH_2N(CH_3)_2$], 126.45, 127.63, 128.01 ($C_{aromatic}$), 142.09 ($C_{q,aromatic}$).

1,3-Bis[(*N,N,N′*-trimethylaminoethyl)aminomethyl]benzene ($L^{Me,Me}$). The ligand $L^{H,H}$ (0.75 g, 2.69 mmol) was mixed with 37% formaldehyde (3.80 mL) and formic acid (4.50 mL), and the resulting mixture was refluxed at 90 °C for 24 h. It was then cooled in an ice bath. A saturated solution of NaOH was added to it with stirring, until the pH of the solution turned 12. The desired product was extracted with $CHCl_3$ (3 × 10 mL). The organic fractions were combined and dried over anhydrous Na_2SO_4. Removal of solvent under reduced pressure afforded yellowish brown oil. Yield: 0.780 g, 93%. Anal. Calcd (%) for $C_{18}H_{34}N_4\cdot 0.15H_2O$: C, 69.92; H, 11.18; N, 18.12. Found: C, 69.98; H, 10.92; N, 18.02. ^{1}H NMR (400 MHz, CD_3CN): δ 2.13 [12H, *s*, $-N(CH_3)_2$], 2.15 (6H, *s*, $-NCH_3$), 2.33−2.48 (8H, *m*, $-NCH_2CH_2N-$), 3.46 (4H, *s*, *m*-xylyl-CH_2N-), 7.15−7.26 (4H, *m*, aromatic protons). ^{13}C NMR (400 MHz, CD_3CN): δ 41.89 ($-NCH_3$), 45.13 ($-N(CH_3)_2$), 55.24 [$-NCH_2CH_2N(CH_3)_2$], 57.44 ($-NCH_2CH_2N(CH_3)_2$), 62.32 (*m*-xylyl-CH_2N-), 127.43, 127.86, 129.41 ($C_{aromatic}$), 139.56 ($C_{q,aromatic}$).

Syntheses of Copper(I) Complexes. $[Cu^I_2(L^{H,H})(MeCN)_4][ClO_4]_2$ (1). To a solution of $[Cu^I(MeCN)_4][ClO_4]$ (0.235 g, 0.720 mmol) in MeCN (3 mL) was added a solution of $L^{H,H}$ (0.100 g, 0.360 mmol) in MeCN (2 mL), under anaerobic conditions. The resulting yellowish brown solution was stirred for 15 min and filtered. The volume of the reaction mixture was reduced to ∼2 mL and degassed Et_2O (30 mL) was added to it with vigorous stirring. This procedure resulted in the separation of an oily mass which was washed several times with Et_2O and dried under a high vacuum to yield an off-white solid. Yield: 0.160 g, 65%. Anal. Calcd (%) for $C_{24}H_{42}Cl_2Cu_2N_8O_8$: C, 37.50; H, 5.51; N, 14.58. Found: C, 37.83; H, 5.30; N, 14.78. IR (KBr, cm^{-1}, selected bands): 3254 [ν(NH)]; 2273 [ν(C≡N)]; 1097, 623 [$\nu(ClO_4^-)$]. ^{1}H NMR (400 MHz, CD_3CN): δ 2.45 [12H, *s*, $-N(CH_3)_2$], 2.55 [4H, *br*, $-HNCH_2CH_2N(CH_3)_2$], 2.75 [4H, *br*, $-HNCH_2CH_2N(CH_3)_2$], 3.81 (4H, *s*, *m*-xylyl-CH_2N-), 7.32−7.46 (4H, *m*, aromatic protons).

$[Cu^I_2(L^{H,H})(PPh_3)_2(MeCN)_2][ClO_4]_2$ (2). To a suspension of $[Cu^I(MeCN)_4][ClO_4]$ (0.235 g, 0.720 mmol) in CH_2Cl_2 (3 mL)

dx.doi.org/10.1021/ic3013848 | *Inorg. Chem.* 2012, 51, 13148−13161

was added a solution of $L^{H,H}$ (0.100 g, 0.360 mmol) in CH_2Cl_2 (3 mL), under anaerobic conditions. After stirring the mixture for 10 min, triphenylphosphine (0.190 g, 0.720 mmol) was added, and stirring was continued for a further 30 min. After filtration (removal of some insoluble material), the volume of the yellowish-brown filtrate was reduced to ~2 mL and degassed Et_2O (30 mL) was added to it, under vigorous magnetic stirring. It resulted in the precipitation of an off-white solid, which was isolated by filtration, washed with Et_2O, and dried in vacuo. Single crystals suitable for X-ray diffraction studies were grown by layering *n*-hexane over a CH_2Cl_2 solution of the off-white product. Yield: 0.290 g, 66%. Anal. Calcd (%) for $C_{56}H_{66}Cl_2Cu_2N_6O_8P_2$: C, 55.54; H, 5.49; N, 6.94. Found: C, 55.60; H, 5.54; N, 6.90. IR (KBr, cm^{-1}, selected bands): 3258 [ν(NH)]; 2268 [ν(C≡N)]; 1095, 621 [$\nu(ClO_4^-)$]. ^{1}H NMR (400 MHz, CD_3CN): δ 2.24 (12H, *s*, $-N(CH_3)_2$), 2.50 [4H, *br*, $-HNCH_2CH_2N(CH_3)_2$], 2.75 (4H, *br*, $-HNCH_2CH_2-$), 3.55 (4H, *s*, *m*-xylyl-CH_2NH-), 7.05–7.49 (34H, *m*, aromatic protons).

$[Cu^I_2(L^{Me,Me})(MeCN)_2][ClO_4]_2$ (3). This complex was synthesized by following a procedure as described for **1**; however, using $L^{Me,Me}$ instead of $L^{H,H}$ as the ligand. Yield: 0.145 g, 62%. Anal. Calcd (%) for $C_{22}H_{40}Cl_2Cu_2N_6O_8$: C, 36.98; H, 5.64; N, 11.76. Found: C, 37.05; H, 5.70; N, 11.70. IR (KBr, cm^{-1}, selected bands): 2274 [ν(C≡N)]; 1093, 624 [$\nu(ClO_4^-)$]. ^{1}H NMR (400 MHz; CD_3CN): δ 2.20 (6H, *s*, $-NCH_3$), 2.40 (12H, *s*, $-N(CH_3)_2$), 2.56 (8H, *br*, $-NCH_2CH_2N-$), 3.79 (4H, *s*, *m*-xylyl-CH_2N-), 7.35–7.46 (4H, *m*, aromatic protons). The PF_6 analogue, **3**·$(PF_6)_2$ was synthesized following a similar procedure using $L^{Me,Me}$ and $[Cu^I(MeCN)_4][PF_6]$ in an inert atmosphere.

$[Cu^I_2(L^{Me,Me})(PPh_3)_2][ClO_4]_2$ (4). This complex was synthesized by following a procedure as described for **2**; however, using $L^{Me,Me}$ instead of $L^{H,H}$ as a ligand. Yield: 0.230 g, 61%. Anal. Calcd (%) for $C_{54}H_{64}Cl_2Cu_2N_4O_8P_2$: C, 56.05; H, 5.58; N, 4.84. Found: C, 56.60; H, 5.64; N, 4.98. IR (KBr, cm^{-1}, selected bands): 1094, 623 [$\nu(ClO_4^-)$]. ^{1}H NMR (400 MHz; CD_3CN): δ 2.17 (6H, *s*, $-NCH_3$), 2.34 [12H, *s*, $-N(CH_3)_2$], 2.54 (8H, *br*, $-NCH_2CH_2N-$), 3.75 (4H, *s*, *m*-xylyl-CH_2N-), δ 7.12–7.48 (34H, *m*, aromatic protons).

Syntheses of Copper(II) Complexes. $[Cu^{II}_2(L^{H,H}-O)(OH)(MeCN)_2][ClO_4]_2$ (5). The ligand $L^{H,H}$ (0.100 g, 0.360 mmol) was dissolved in dinitrogen-flushed MeCN (10 mL). To it, solid $[Cu^I(MeCN)_4][ClO_4]$ (0.235 g, 0.720 mmol) was added, under positive dinitrogen pressure. The resulting yellowish-brown solution was stirred for 15 min, and then it was exposed to dry dioxygen, resulting in a color change from initial green to bluish green. After 2 h of stirring, slow diffusion of EtOAc to the solution resulted in the formation of a green crystalline solid. The green solid was collected by filtration, washed with a mixture of MeCN-EtOAc (1:5, v/v), and dried in vacuo. Yield: 0.210 g, 81%. Single crystals suitable for X-ray analysis were obtained by diffusion of EtOAc into a MeCN solution of the complex. Anal. Calcd (%) for $C_{20}H_{36}Cl_2Cu_2N_6O_{10}$: C, 33.43; H, 5.05; N, 11.70. Found: C, 33.21; H, 5.19; N, 11.25. Conductivity (MeCN, 10^{-3} M solution at 298 K): Λ_M = 290 Ω^{-1} cm^2 mol^{-1} (expected range[45] for 1:2 electrolyte: 220–300 Ω^{-1} cm^2 mol^{-1}). IR (KBr, cm^{-1}, selected bands): 3420 [ν(OH)], 3262 [ν(NH)], 1309 [ν(Ph–O)], 1085, 623 [$\nu(ClO_4^-)$]. Electronic spectrum [λ_{max}, nm (ε, $M^{-1}cm^{-1}$)] (in MeCN): 600 (180), 360 (2220), 335 (2200), 245 (11550).

Reaction of $L^{Me,Me}$ with Copper(I) and Subsequent Oxygenation. Synthesis of $[Cu^{II}_2(L^{Me,Me}-O)(OH)(OClO_3)][ClO_4]$·MeCN (6). The reactions were carried out in three different solvents (MeCN, MeOH, and CH_2Cl_2) by using the same amount of ligand $L^{Me,Me}$ and $[Cu^I(MeCN)_4][ClO_4]$ and by following a similar procedure. The case in CH_2Cl_2 is described below.

To a dinitrogen-flushed solution of $L^{Me,Me}$ (0.100 g, 0.327 mmol) in CH_2Cl_2 (10 mL), solid $[Cu^I(MeCN)_4][ClO_4]$ (0.213 g, 0.654 mmol) was added, under positive dinitrogen pressure at 298 K. The resulting yellow suspension of an extremely air-sensitive dicopper(I) complex was stirred for 10 min, under a dinitrogen atmosphere, and finally exposed to dioxygen. After stirring for ~24 h, a blue solid precipitated out from the green solution. The blue solid was collected by filtration, washed several times by CH_2Cl_2, and vacuum-dried. Yield: 0.160 g {74%, based on the composition $[Cu^{II}_2(L^{Me,Me})(OH)_2][ClO_4]_2$ (**7**)}. Solvent was removed from the green filtrate, and the solid thus obtained was dissolved in MeCN. Slow diffusion of EtOAc to such a solution resulted in the formation of a green crystalline complex. Single crystals thus obtained were found to be suitable for X-ray structural studies. Yield: 0.050 g {22%, based on the composition $[Cu^{II}_2(L^{Me,Me}-O)(OH)(OClO_3)][ClO_4]$·MeCN (**6**)}. The yields of the green solid in various solvents are as follows: MeCN, 0.190 g (82%); MeOH, 0.140 g (60%).

Characterization of Dicopper(II) Complexes. Green Solid. Anal. Calcd (%) for $[Cu^{II}_2(L^{Me,Me}-O)(OH)(OClO_3)][ClO_4]$·MeCN (**6**), $C_{20}H_{37}Cl_2Cu_2N_5O_{10}$: C, 34.05; H, 5.29; N, 9.93. Found: C, 34.39; H, 5.45; N, 10.05. Conductivity (MeCN, 10^{-3} M solution at 298 K): Λ_M = 300 Ω^{-1} cm^2 mol^{-1}. IR (KBr, cm^{-1}; selected bands): 3437 [ν(OH)], 1315 [ν(Ph–O)], 1095, and 623 [$\nu(ClO_4^-)$]. Electronic spectrum [λ_{max}, nm (ε, M^{-1} cm^{-1})] (in MeCN): 607 (190), 372 (2350), 330 sh (2060), 264 (13 450).

Blue Solid. Anal. Calcd (%) for $[Cu^{II}_2(L^{Me,Me})(OH)_2][ClO_4]_2$ (**7**), $C_{18}H_{36}Cl_2Cu_2N_4O_{10}$: C, 32.43; H, 5.41; N, 8.41. Found: C, 32.46; H, 5.81; N, 8.07. Conductivity (MeCN, 10^{-3} M solution at 298 K): Λ_M = 280 Ω^{-1} cm^2 mol^{-1}. IR (KBr, cm^{-1}; selected bands): 3578 [ν(OH)], 1093, and 624 [$\nu(ClO_4^-)$]. Electronic spectrum [λ_{max}, nm (ε, $M^{-1}cm^{-1}$)] (in MeCN): 615 (235), 370 weak sh (500), 270 (8150). MALDI {2-[(2*E*)-3-(4-*tert*-butylphenyl)-2-methylprop-2-enylidene]malononitrile as matrix, in MeCN}: *m*/*z* 563.1 ($\{[Cu^{II}_2(L^{Me,Me})(OH)_2][ClO_4]\} - 2H^+ - 2e^-)^+$.

Physical Measurements. Elemental analyses (C, H, N) were obtained using Thermo Quest EA 1110 CHNS-O. Conductivity measurements were done with an Elico type CM-82T conductivity bridge (Hyderabad, India). Spectroscopic measurements were made using the following spectrometers: Bruker Vector 22 (IR: KBr, 4000–500 cm^{-1}), Agilent 8453 diode-array (UV–vis), Waters-HAB213 spectrometer (ESI-MS), Bruker Autoflex (MALDI) (ICIQ, Tarragona, Spain). ^{1}H and ^{13}C NMR spectra were obtained on JEOL JNM LA 400 (400 MHz) NMR spectrometer. Chemical shifts are reported in parts per million referenced to TMS. Low-temperature absorption spectra at a high concentration of complex {[**3**·$(CF_3SO_3)_2$] ~ 1 mM} were recorded by a dip-probe technique [Ocean Optics, TP300-UV–vis Transmission Dip Probe; path length was adjusted to 2 mm by using RTP-2-10 (adjustable 2-10 mm) transmission tip] at 193 K, in tetrahydrofuran (THF). The 193 K temperature was attained by mixing liquid dinitrogen into MeOH in a dewar flask. The spectra at a low concentration of the complex {[**3**·$(X)_2$] ~ 0.1 mM; X = CF_3SO_3, PF_6} were recorded by an Agilent 8453 diode-array UV–vis spectrometer, equipped with an Unisoku Unispeks cryostat using 1 cm quartz cuvette at 183 K in THF and acetone.

Variable-temperature magnetic susceptibility measurements in the solid state of **5** and **6** were performed in the temperature range of 50–300 K, with a Quantum Design SQUID magnetometer (València, Spain). Susceptibilities were corrected for diamagnetic contributions. Effective magnetic moments were calculated using μ_{eff} = 2.828-$[\chi_M T]^{1/2}$, where χ_M is the corrected[46] molar susceptibility. Solution-state magnetic susceptibilites on **5** and **6** were obtained by the NMR technique of Evans[47] in MeCN with a JEOL JNM LA 400 (400 MHz) NMR spectrometer and made use of the paramagnetic shift of the methyl protons of the MeCN reference as the measured NMR parameter.

Cyclic voltammetric measurements were performed using CH Instruments Electrochemical Analyzer/Workstation Model 600B Series. A standard three-electrode cell was employed with a Beckman (M-39273) platinum-inlay working electrode, a platinum-wire auxiliary electrode, and a saturated calomel electrode (SCE) as a reference; no correction was made for the junction potential. Potentials were recorded at 25 °C. The concentrations of solute and $[^nBu_4N][ClO_4]$ were ~1.0 mM and 0.1 M, respectively.

Crystal Structure Determination. X-ray data were collected on a Bruker SMART APEX CCD diffractometer, with graphite-monochromated Mo–Kα (λ = 0.71073 Å) radiation. The data for complex **2** were collected at 293(2) K, whereas for complexes **5** and **6**, the data were collected at 100(2) K. For data reduction a "Bruker Saint Plus"

Table 1. Data Collection and Structure Refinement Parameters for $[Cu^{I}_2(L^{H,H})(PPh_3)_2(MeCN)_2][ClO_4]_2$ (2), $[Cu^{II}_2(L^{H,H}-O)(OH)(MeCN)_2][ClO_4]_2$ (5), and $[Cu^{II}_2(L^{Me,Me}-O)(OH)(OClO_3)][ClO_4]\cdot MeCN$ (6)

	2	5	6
chemical formula	$C_{56}H_{64}Cl_2Cu_2N_6O_8P_2$	$C_{20}H_{36}Cl_2Cu_2N_6O_{10}$	$C_{20}H_{37}Cl_2Cu_2N_5O_{10}$
formula weight	1209.05	718.53	705.53
crystal color, habit	white, block	green, block	green, block
temperature (K)	293(2)	100(2)	100(2)
λ (Å)	Mo Kα (0.71073)	Mo Kα (0.71073)	Mo Kα (0.71073)
crystal system	monoclinic	monoclinic	monoclinic
crystal size/ (mm × mm × mm)	0.2 × 0.2 × 0.2	0.2 × 0.2 × 0.2	0.2 × 0.2 × 0.2
space group	*Pn* (no. 7)	$P2_1$ (no. 4)	$P2_1/n$ (no. 14)
a (Å)	16.701(5)	7.485(5)	9.349(5)
b (Å)	9.905(5)	14.760(5)	16.584(5)
c (Å)	18.435(5)	13.570(5)	18.245(5)
α(°)	90.0	90.0	90.0
β(°)	107.712(5)	104.648(5)	90.672(5)
γ(°)	90.0	90.0	90.0
V/(Å^3)	2905.0(19)	1450.5(12)	2828.6(19)
Z	2	2	4
D_c (g cm^{-3})	1.382	1.645	1.657
μ (mm^{-1})	0.936	1.711	1.752
reflections measured	18885	9720	18531
unique reflections (R_{int})	11466 (R_{int} = 0.0837)	5728 (R_{int} = 0.0254)	6973 (R_{int} = 0.0540)
No. of reflections used [$I > 2\sigma(I)$]	5688	5384	4799
No. of parameters	687	375	357
final *R* indices	$^aR_1$ = 0.0834	$^aR_1$ = 0.0335	$^aR_1$ = 0.0609
	$^bwR_2$ = 0.1624	$^bwR_2$= 0.0723	$^bwR_2$= 0.1324
R indices (all data)	$^aR_1$ = 0.1712	$^aR_1$ = 0.0361	$^aR_1$ = 0.0928
	$^bwR_2$ = 0.1979	$^bwR_2$= 0.0734	$^bwR_2$= 0.1463
goodnes-of-fit on F^2	0.922	1.005	0.974

$^aR_1 = \Sigma(|F_o| - |F_c|)/\Sigma|F_o|$. $^bwR_2 = \{\Sigma[w(|F_o|^2 - |F_c|^2)^2]/\Sigma[w(|F_o|^2)^2]\}^{1/2}$.

program was used. Data were corrected for Lorentz and polarization effects; an empirical absorption correction (SADABS) was applied. Structures were solved by SIR-97 and refined by full-matrix least-squares methods based on F^2 using SHELXL-97, incorporated in a WinGX 1.64 crystallographic collective package.[48] For **2**, **5**, and **6**, all non-hydrogen atoms were refined anisotropically. For **5**, three hydrogen atoms and for **6**, one hydrogen atom was located from difference in the Fourier map; the positions of all other hydrogen atoms for **2**, **5**, and **6** were calculated assuming ideal geometries. During refinement, bond restraints were applied to the bonds N(2)−H(21) and O(2)−H(23) of complex **5** to obtain reasonable bond lengths. For **6**, an unassigned peak (1.861 Å^3) was found near the Cu(2) atom at a distance of 0.862 Å, which may be due to the poor quality of crystal chosen for data collection. Pertinent crystallographic parameters of complexes **2**, **5**, and **6** are summarized in Table 1.

Kinetic Experiments. The kinetic studies related to the bis(μ-oxo)dicopper(III) intermediate species (its formation, thermal decay, and reactivity with 2,4-di-*tert*-butylphenolate) were monitored spectrophotometrically using an Agilent 8453 diode-array UV−vis spectrometer, equipped with an Unisoku Unispeks cryostat using a 1 cm quartz cuvette at 183 K in THF with $[\mathbf{3}\cdot(PF_6)_2] \sim 0.1$ mM.

Catechol oxidase activities of complexes **5**, **6**, $[Cu^{II}_2(L^1-O)(OH)(OClO_3)_2]\cdot 1.5H_2O$ (**8**),[28] and $[Cu^{II}_2(L^2-O)(OH)(OClO_3)][ClO_4]$ (**9**)[30,31] were studied in dioxygen-saturated MeOH at 303 K by reaction of the complexes with 3,5-di-*tert*-butylcatechol (3,5-DTBC). Kinetic experiments for the oxidation of 3,5-DTBC were monitored spectrophotometrically using an Agilent 8453 diode-array spectrophotometer, equipped with a 89090A temperature-controller. Increase of the characteristic absorption band of the product 3,5-di-*tert*-butyl-*o*-benzoquinone (3,5-DTBQ) at ~400 nm was monitored as a function of time. In a typical experiment, 2.5 mL of a complex solution in dioxygen-saturated MeOH ($[Complex]_i = 2.60 \times 10^{-5}$ M) was taken in a 1 cm quartz cell, and the reaction was initiated by the addition of 0.1 mL of catechol solution ($[3,5\text{-DTBC}]_i = 1.625 \times 10^{-3}$ to 3.250×10^{-2} M). In a separate set of experiments, the kinetic determinations were performed without the catalyst. Initial rates were determined from the slope of the tangent to the absorbance versus the time curve at $t = 0$. The conversion of the reaction rate was done using ε = 1900 M^{-1} cm^{-1} for 3,5-DTBQ in MeOH.[32] A kinetic treatment on the basis of the Michaelis−Menten approach was applied, and the results were evaluated from the Lineweaver−Burk double-reciprocal plots. Experiments to determine the dependence of the reaction rate on the complex concentration were carried out at 303 K: $[3,5\text{-DTBC}]_f = 1.25 \times 10^{-3}$ M, $[complex]_f = 2.50 \times 10^{-5}$ to 12.50×10^{-5} M.

Detection of Hydrogen Peroxide in the Catalytic Reactions. The formation of H_2O_2 during the catalytic reaction was detected by following the development of the characteristic band for I_3^- spectrophotometrically (λ_{max} = 353 nm; ε = 26 000 M^{-1} cm^{-1}), upon reaction with I^-.[36,37] The oxidation reactions of 3,5-DTBC in the presence of different catalysts were carried out as in the kinetic experiments ($[Complex]_f = 2.5 \times 10^{-5}$ M; $[3,5\text{-DTBC}]_f = 50 \times 10^{-5}$ M), and after 1 h, the reaction was quenched by adding an equal volume of H_2SO_4 (20×10^{-3} M). The quinone formed was extracted three times with CH_2Cl_2. One milliliter of 10% aqueous KI solution was added to the aqueous layer. In order to accelerate the formation of I_3^- in the presence of H_2O_2, ammonium molybdate (3%) solution was added in a catalytic amount.[38b] In the presence of H_2O_2, a band due to the formation of I_3^- developed. Since atmospheric dioxygen can oxidize I^-, blank experiments (without catalyst or without 3,5-DTBC) were also performed. For the catalytic reactions performed in the presence of **5**, **6**, **8**, and **9**, an appreciable H_2O_2 formation was found. However, only minor formation of the I_3^- band was observed during the blank test.

Oxidation of 2,4-Di-*tert*-butylphenolate by Bis(μ-oxo)-dicopper(III) Species of $L^{Me,Me}$. The *O* species (2 mM, 5 mL) was generated by injecting $\mathbf{3}\cdot(PF_6)_2$ into an oxygen-saturated THF at

dx.doi.org/10.1021/ic3013848 | *Inorg. Chem.* 2012, 51, 13148−13161

183 K. The yellow-green species was allowed to fully form over 10 min, and then excess dioxygen was removed prior to addition of the substrate by bubbling N_2 for 10 min. The reaction with 2,4-di-*tert*-butylphenolate was performed at 183 K. Addition of 2 equiv of the substrate brought about a change in color from yellow-green to green. After 2 h, the reaction mixture was quenched with H_2SO_4 (1M, 2 mL). After solvent removal, the residue was extracted with CH_2Cl_2, and the products were analyzed and quantified by ^{1}H NMR.

RESULTS AND DISCUSSION

Syntheses of Ligands and Dicopper(I) Complexes. Considerable progress has been made in the chemical modeling of tyrosinase[19−21,22a,b,23−28] and the use of phenoxo- and hydroxo-bridged dicopper(II) complexes as models for the *met* form of catechol oxidase.[32a,33,34,38d,40,43] Studies of the reactivity of molecular oxygen with dicopper(I) complexes of designed ligands that model tyrosinase-like monooxygenase activity (intramolecular aromatic ring hydroxylation) have used *m*-xylyl-based dinucleating ligands, providing di/trinitrogen terminal coordination.[19−21,22a,b,23−28] Karlin and co-workers reported the first model[22a,b] to demonstrate the binding and activation of molecular oxygen to chemically model aromatic ring hydroxylation reaction of pertinence to tyrosinase, and there is good evidence for a ($\mu-\eta^2:\eta^2$-peroxo)dicopper(II) (side-on peroxo) intermediate to bring about xylyl-ring hydroxylation.[22c] The influence of ligand topology in the modeling of such reactions is of great importance in order to elucidate the detailed pathways that can lead to the activation of the molecular oxygen by copper(I) complexes toward the oxidation of C−H bonds, and therefore has implications in the understanding of metalloenzymes and other catalysts.[14d,49]

The ligands $L^{H,H}$ and $L^{Me,Me}$ (Figure 1) were considered primarily to investigate the formation and stability of the intermediate species, as copper(I) complexes of peralkylated aliphatic amines are known to stabilize both ***O*** and ***P*** isomers when reacted with dioxygen at low temperatures.[14c,15a] We reasoned that if an ***O*** or ***P*** intermediate is formed whether or not xylyl-ring hydroxylation reaction would take place.

m-Xylyl-based binucleating ligand, $L^{H,H}$, is synthesized by Schiff base condensation between isophthalaldehyde and *N*,*N*-dimethylethylenediamine in EtOH,[28] followed by reduction with $NaBH_4$ in MeOH.[19d,28] Subsequent N-methylation of $L^{H,H}$ by $HCHO/HCO_2H$[19d] affords $L^{Me,Me}$. Both $L^{H,H}$ and $L^{Me,Me}$ have been characterized by ^{1}H and ^{13}C NMR spectra (Figures S1−S4 of the Supporting Information) and elemental analyses. Treatment of $L^{H,H}$ and $L^{Me,Me}$ with two equiv of $[Cu^I(MeCN)_4][ClO_4]$ in MeCN, under anaerobic conditions, led to the isolation of air-sensitive binuclear copper(I) complexes $[Cu^I_2(L^{H,H})(MeCN)_4][ClO_4]_2$ (**1**) and $[Cu^I_2(L^{Me,Me})(MeCN)_2][ClO_4]_2$ (**3**), respectively. The presence of coordinated MeCN was confirmed from their IR spectra [a weak absorption at ∼2270 cm^{-1} due to the ν(C≡N) stretching vibration]. IR spectra also displayed the presence of an uncoordinated perchlorate counterion. In spite our repeated attempts, unfortunately we could not grow single crystals of **1** and **3** for structural analysis. Because of its π-acceptor property, PPh_3 stabilizes the lower oxidation state of metal ions, and therefore attempts were made to synthesize and grow single crystals of the corresponding copper(I)−phosphine complexes, for structural analysis. Thus, treatment of $L^{H,H}$ and $L^{Me,Me}$ with $[Cu^I(MeCN)_4][ClO_4]$ and PPh_3 afforded the complexes $[Cu^I_2(L^{H,H})(PPh_3)_2(MeCN)_2][ClO_4]_2$ (**2**) and $[Cu^I_2(L^{Me,Me})(PPh_3)_2][ClO_4]_2$ (**4**), respectively. IR spectra confirmed the presence of both MeCN and perchlorate counterion in **2** and only perchlorate counterion in **4**. Although we were successful in growing single crystals of **2** for its structural characterization, we have been unsuccessful thus far in the case of **4**. Since copper(I) has d^{10} electronic configuration, the Cu^I complexes **1**−**4** are diamagnetic, as indicated by their ^{1}H NMR spectra in CD_3CN (Figures S5−S8 of the Supporting Information). On the basis of comparisons with free ligands, the observed resonances have been assigned. As is found for similar cases, the predominating tendency is for a downfield shift of ^{1}H resonances upon coordination to the positively charged metal ion (coordination-induced shift).[50] Elemental analyses, IR, and ^{1}H NMR spectral data are in good agreement with the above formulations for all the copper(I) complexes.

Reactivity of 1 and 3 with Dioxygen at Room Temperature and Product Identification. Exposure of "solution-generated" dicopper(I) complexes **1** and **3** with molecular oxygen in MeCN at room temperature (298 K) brings about a noticeable color change from pale yellow to green. In the framework of our research work dealing with isolation and characterization of products due to the reaction between copper(I) complexes and dioxygen,[19] during workup of green MeCN solutions in air we isolated two dicopper(II) complexes of composition $[Cu^{II}_2(L^{H,H}-O)(OH)(MeCN)_2][ClO_4]_2$(**5**) and $[Cu^{II}_2(L^{Me,Me}-O)(OH)(OClO_3)][ClO_4]\cdot MeCN$(**6**). The phenoxo- and hydroxo-bridged dicopper(II) complexes **5** and **6** have been structurally characterized (see below), demonstrating that the tailor-made ligands, $L^{H,H}$ and $L^{Me,Me}$, support the xylyl-ring hydroxylation reaction.

Notably, while the works of Karlin,[14d,22c] Tolman,[23] and others[25] have clearly established the intermediacy of ***P*** species in carrying out *m*-xylyl-ring hydroxylation, the association of an ***O*** intermediate with an aromatic ring hydroxylation is much more limited.[9] To the best of our knowledge, it has not been documented for any arene self-hydroxylating *m*-xylyl system. From this perspective, the low-temperature absorption spectroscopic detection of the ***O*** species with *m*-xylyl-based ligand, $L^{Me,Me}$, and decay of the putative intermediate with subsequent xylyl-ring hydroxylation is a noteworthy result.

IR spectra of **5** and **6** display absorptions due to ν(O−H) at ∼3430 cm^{-1} and $\nu(ClO_4^-)$ at ∼1100 and ∼620 cm^{-1}. Complexes **5** and **6** display an additional strong absorption at ∼1300 cm^{-1}, typical for ν(C−O) vibration of the coordinated phenolate.[19] This is absent in the corresponding dicopper(I) complexes **1** and **3**, as expected. An easy means of identifying the complexes is their electronic spectral features. The electronic spectra of **5** and **6** in MeCN are displayed in Figures S9 and S10 of the Supporting Information, respectively. Crystal-field transitions at 600 nm (ε = 180 M^{-1} cm^{-1}) for **5** and 607 nm (ε = 190 M^{-1} cm^{-1}) for **6** are observed. Intense ligand-to-metal charge-transfer (LMCT) bands due to $PhO^-\rightarrow Cu^{II}$ and/or $OH^-\rightarrow Cu^{II}$ are also observed: at 360 nm (ε = 2220 M^{-1} cm^{-1}) and 335 nm (ε = 2200 M^{-1} cm^{-1}) for **5** and at 372 nm (ε = 2350 M^{-1} cm^{-1}), along with a shoulder at 330 nm (ε = 2060 M^{-1} cm^{-1}), for **6**. Similar spectral features are characteristic of phenoxo- and hydroxo-bridged dicopper(II) complexes.[19d,e,22a,b,23,28]

Notably, exposure of "solution-generated" dicopper(I) complex **3** in CH_2Cl_2 at room temperature with molecular oxygen afforded a green solution along with a blue precipitate. It should be noted, however, that no blue solid was observed when the experiment was done in MeCN. The formation of

dx.doi.org/10.1021/ic3013848 | *Inorg. Chem.* 2012, 51, 13148−13161

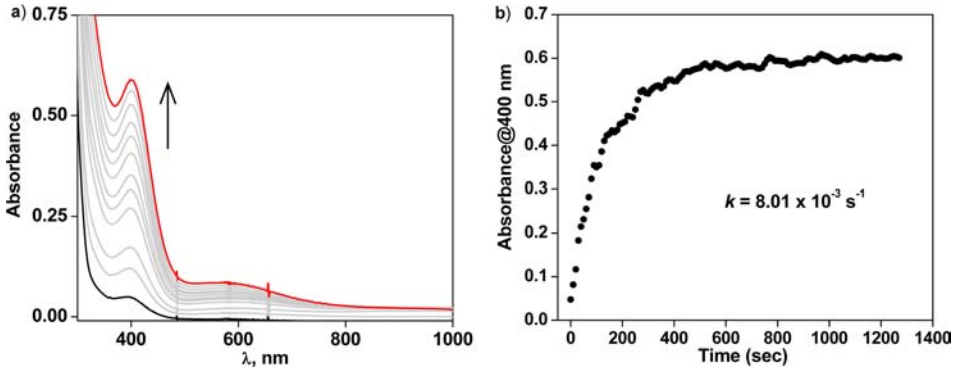

Figure 2. (a) UV−vis spectra of the formation of bis(μ-oxo)dicopper(III) species in the reaction of **3**·$(PF_6)_2$ (~ 0.1 mM) with O_2 in THF at 183 K. (b) Time trace of absorbance at 400 nm.

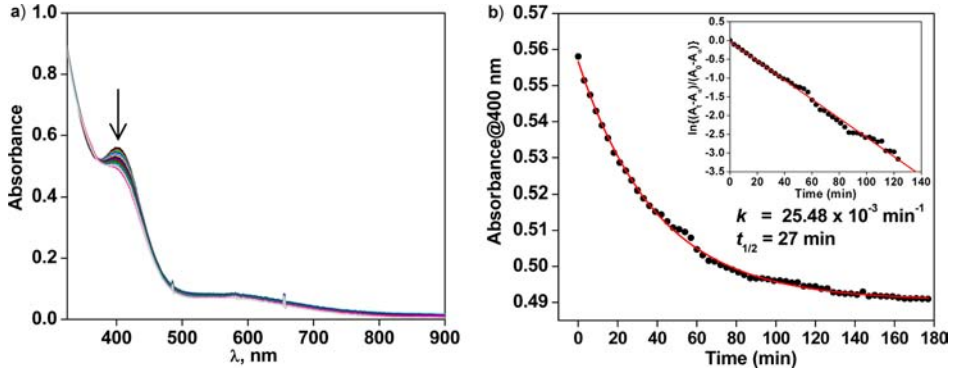

Figure 3. (a) Spectral change due to the thermal decay of the bis(μ-oxo)dicopper(III) species of $L^{Me,Me}$ at 203 K in THF during a 3 h period. (b) Time trace of absorbance at 400 nm; inset: rate plot.

this blue solid [unhydroxylated oxidation product $[Cu^{II}_2(L^{Me,Me})(OH)_2][ClO_4]_2$ (**7**), see below] could be explained by competition for the inter- rather than the intramolecular O_2-binding processes when dicopper(I) complex **3** reacts with O_2, apparently favored in nonpolar CH_2Cl_2 compared to a polar MeCN medium. Similar observations were noticed before.[23,51] IR spectrum of the blue solid displays a broad band at ~3600 cm^{-1} due to the coordinated water and/or hydroxo group. The presence of an ionic perchlorate is confirmed from absorptions observed at ~1100 and ~620 cm^{-1}. It is to be noted that for this blue solid, no IR absorption due to ν(C−O) is observed, implying that it is not a xylyl ring-hydroxylated product (Figure S11 of the Supporting Information). Crystal-field transition at 615 nm (ε = 235 M^{-1} cm^{-1}) is observed. A ligand-to-metal charge-transfer (LMCT) band due to $OH^- \rightarrow Cu^{II}$ is observed as a weak shoulder at 370 nm (ε = 500 M^{-1} cm^{-1}). Similar spectral features are characteristic of dihydroxo-bridged dicopper(II) complexes.[19d,e] ^1H NMR spectral analysis of copper(II)-removed organic compound from blue complex (see below) confirms that the organic ligand, $L^{Me,Me}$, remains intact during the oxygenation experiment.

Taken together, in the above results and physicochemical data [elemental analysis and solution electrical conductivity (1:2 electrolyte)], we identify the blue product as the bis(μ-hydroxo)dicopper(II) complex $[Cu^{II}_2(L^{Me,Me})(OH)_2][ClO_4]_2$ (**7**). MALDI-MS spectrum of complex **7** (an intense peak was observed at m/z value of 563.1 corresponding to the species $(\{[Cu^{II}_2(L^{Me,Me})(OH)_2][ClO_4]\} - 2H^+ - 2e^-\}^+)$ is displayed in Figure S12 of the Supporting Information. The effective magnetic moment (μ_{eff}/Cu) value of **7** in the solid state at 27 °C was determined to be 1.44 μ_B, indicative of the presence of antiferromagnetically coupled dicopper(II) centers.[19d,e] The observed μ_{eff}/Cu value is typical for dihydroxy-bridged dicopper(II) complexes.[19d,e] Unfortunately, all our attempts to grow single crystals of **7** suitable for structural analysis have so far been unsuccessful.

Reactivity of the Dicopper(I) Complex of $L^{Me,Me}$ Toward Dioxygen at Low Temperature. To investigate the possibility of the formation of a "Cu_2O_2" intermediate, the reactivity study of the dicopper(I) complex of $L^{Me,Me}$ with dioxygen was performed at low temperature. The Cu_2O_2 intermediate was generated by injecting THF solution of $[Cu^I(MeCN)_4][CF_3SO_3]$ into a dioxygen-saturated THF solution of $L^{Me,Me}$, equilibrated at 193 K, in a 2:1 ratio with a final concentration of ~1 mM. A yellowish-green species generated within a minute. To throw light on the nature of the intermediate formed (see below) low-temperature UV−vis spectral studies were performed, as authentic copper−oxygen species have characteristic absorption spectroscopic signatures.[6−18] The spectrum is displayed in Figure S13 of the Supporting Information. Two absorption bands at 315 nm (ε ~6500 M^{-1} cm^{-1}) and at 400 nm (ε ~ 8500 M^{-1} cm^{-1}) developed. The spectral feature of this intermediate species formed is quite similar to those of the reported bis(μ−oxo)dicopper(III) intermediate.[14,15,29,52] The formation of the ***O*** species was also examined at a low concentration of the complex (~0.1 mM) by injecting **3**·$(X)_2$ (X = $CF_3SO_3^-$, PF_6^-) into an oxygen-saturated THF and acetone at 183 K. The intermediate formation is invariant of the counteranion used. The UV−vis spectra for the PF_6^- counteranion in THF and in acetone are displayed in Figure S14 of the Supporting Information.

dx.doi.org/10.1021/ic3013848 | Inorg. Chem. 2012, 51, 13148−13161

Scheme 1. Product Analysis Due to Reaction between the Bis(μ-oxo)dicopper(III) Intermediate of $L^{Me,Me}$ and 2,4-Di-*tert*-butylphenolate in THF at 183 K

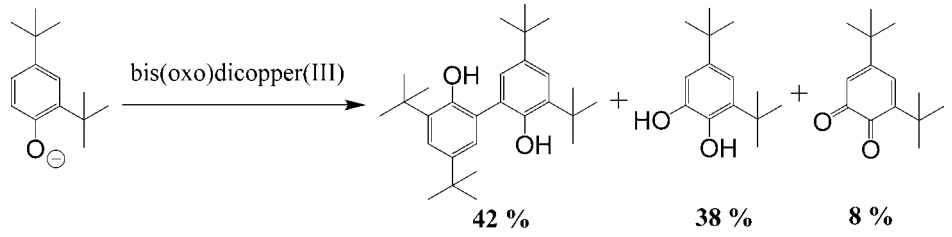

UV−vis spectra of the formation of the ***O*** species due to the reaction of **3**·$(PF_6)_2$ (~0.1 mM) with O_2 in THF at 183 K and the time trace of absorbance at 400 nm are displayed in Figure 2. The first-order formation constant, $k = 8.01 \times 10^{-3}$ s^{-1}, is estimated. UV−vis spectra of **3**·$(PF_6)_2$, bis(μ-oxo)dicopper(III) species of $L^{Me,Me}$ at 183 K, and the decay product at room temperature in THF are displayed in Figure S15 of the Supporting Information.

The kinetics of thermal decomposition of the bis(μ-oxo)dicopper(III) species was studied by monitoring the decay of the 400 nm band at various temperatures (203−233 K) in THF. The ***O*** species was first generated at 183 K, and after its full formation, the temperature was raised by a temperature controller to the desired value. Data collection for the decay started only after the solution had attained the desired temperature (~2−3 min was required to attain thermal equilibrium). Spectral changes due to thermal decay of the ***O*** species at 203 K in THF during the 3 h period and a time trace of the absorbance of 400 nm are displayed in Figure 3. The values of k were determined at different temperatures and activation parameters; $\Delta H^{\#}$ and $\Delta S^{\#}$ were obtained from the Eyring plot, Figure S16 of the Supporting Information. The following values were obtained: $\Delta H^{\#} = 23.42$ kJ mol^{-1}; $\Delta S^{\#} = -190$ J K^{-1} mol^{-1}. The activation parameters obtained are comparable to that obtained by others.[12,23]

Reactivity of Bis(μ-oxo)dicopper(III) Species of $L^{Me,Me}$ with Externally Added Phenolate. To investigate whether or not the ***O*** species of $L^{Me,Me}$ has the potential to hydroxylate an externally added substrate, we examined its reactivity with 2,4-di-*tert*-butylphenolate. UV−vis spectra of the ***O*** species (0.1 mM) after addition of 2 equiv of 2,4-di-*tert*-butylphenolate (0.2 mM), the spectra after 1 h, and the decay profile of ***O*** species due to reaction with 2,4-di-*tert*-butylphenolate in THF at 183 K are displayed in Figure S17 of the Supporting Information. The products have been identified by ^{1}H NMR spectral analysis (Figure S18 of the Supporting Information). Notably, three products could be identified (Scheme 1): C−C-coupled dimer (42%), 3,5-di-*tert*-butylcatechol (38%), and 3,5-di-*tert*-butyl-*o*-benzoquinone (8%). The ESI-MS data also confirms the formation of the three products. Among other products, hydroxylation of phenolate occurs (however, no intramolecular ligand hydroxylation was observed in the THF solvent). The result presented here is of significance given the fact that the ligand $L^{Me,Me}$ not only stabilizes the bis(μ-oxo)dicopper(III) core but also exhibits both intramolecular xylyl-ring hydroxylation (see below) and hydroxylation of the externally added substrate, 2,4-di-*tert*-butylphenolate, generating the catechol and quinone of pertinence to tyrosinase-like activity.

Notably, while the works of Karlin,[14d,22c] Tolman,[23] and others[25] have clearly established the intermediacy of ***P*** species in carrying out *m*-xylyl-ring hydroxylation, association of the ***O*** intermediate with aromatic ring hydroxylation is much more limited.[9] To the best of our knowledge, it has not been documented for any arene self-hydroxylating *m*-xylyl system. From this perspective, the low-temperature absorption spectroscopic detection of the ***O*** species with *m*-xylyl-based ligand, $L^{Me,Me}$, and decay of the putative intermediate with subsequent xylyl-ring hydroxylation is a noteworthy result.

Solvent Dependence of Aromatic Ring Hydroxylation. The role of the solvent is expected to be of significance, since the availability of the open-coordination site is dependent on the coordinating ability of the solvent. Moreover, the stability of the dioxygen adduct is expected to be influenced by the interaction between the dioxygen adduct and the solvent.[19d] The extent of the aromatic-ring hydroxylation product in the reaction of copper(I) complexes of $L^{Me,Me}$ with dioxygen depends on the nature of the medium in which the synthetic reactions have been performed. The formation of the phenoxo- and hydroxo-bridged dicopper(II) complex, the aromatic ring-hydroxylated product, varied with the polarity of the solvent. The reaction resembles a simple electrophilic aromatic substitution and might be expected to proceed via a cationic intermediate akin to a "σ complex" that would be preferentially stabilized in a polar solvent.[19d] In polar solvents like MeCN (dielectric constant, $\varepsilon = 37.5$), the extent of hydroxylation was almost quantitative, which decreased in a comparatively less polar MeOH ($\varepsilon = 32.6$) and was considerably less in a nonpolar solvent like CH_2Cl_2 ($\varepsilon = 9.1$). A similar trend was observed before from this laboratory.[19d,28]

Description of Structures. (a)$[Cu^I_2(L^{H,H})(PPh_3)_2(MeCN)_2][ClO_4]_2$ (2). A perspective view of the cationic part of **2** is shown in Figure 4. Selected bond lengths and bond angles are collected in Table 2. The structure of the ligand $L^{H,H}$, its bis-bidentate mode of coordination, and the binding of PPh_3 and MeCN in **2** are confirmed. The four coordination of each copper(I) center is satisfied by three nitrogen donor atoms (two of which originate from the *N*,*N*-dimethylethylenediamine moiety of $L^{H,H}$ and one from acetonitrile) and PPh_3.

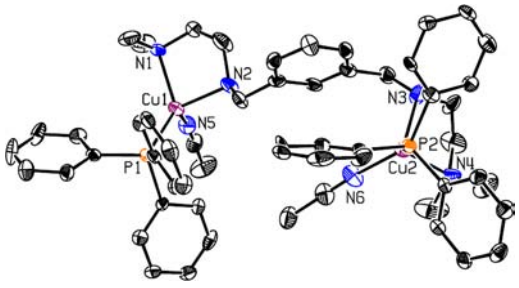

Figure 4. Perspective view of the metal coordination environment in the crystal of $[Cu^I_2(L^{H,H})(PPh_3)_2(MeCN)_2][ClO_4]_2$ (**2**). Only donor atoms are labeled. Hydrogen atoms are omitted for clarity.

dx.doi.org/10.1021/ic3013848 | *Inorg. Chem.* 2012, 51, 13148−13161

Table 2. Selected Bond Distances (Å) and Bond Angles (°) in the Cationic Part of $[Cu^{I}_2(L^{H,H})(PPh_3)_2(MeCN)_2][ClO_4]_2$ (2), $[Cu^{II}_2(L^{H,H}-O)(OH)(MeCN)_2][ClO_4]_2$ (5), and $[Cu^{II}_2(L^{Me,Me}-O)(OH)(OClO_3)][ClO_4]\cdot MeCN$ (6)

2		5		6	
Cu(1)–N(1)	2.128(7)	Cu(1)–N(1)	2.015(3)	Cu(1)–N(1)	2.012(4)
Cu(1)–N(2)	2.122(8)	Cu(1)–N(2)	1.996(3)	Cu(1)–N(2)	1.993(4)
Cu(1)–N(5)	2.034(9)	Cu(1)–N(5)	2.432(3)	Cu(1)–O(1)	1.932(3)
Cu(1)–P(1)	2.178(3)	Cu(1)–O(1)	1.944(2)	Cu(1)–O(2)	1.896(3)
Cu(2)–N(3)	2.136(9)	Cu(1)–O(2)	1.933(2)	Cu(2)–N(3)	1.998(4)
Cu(2)–N(4)	2.130(9)	Cu(2)–N(3)	1.993(3)	Cu(2)–N(4)	2.007(4)
Cu(2)–N(6)	1.972(9)	Cu(2)–N(4)	2.026(3)	Cu(2)–O(1)	1.934(3)
Cu(2)–P(2)	2.178(3)	Cu(2)–N(6)	2.336(3)	Cu(2)–O(2)	1.897(3)
Cu(1)···Cu(2)	8.507(3)	Cu(2)–O(1)	1.963(2)	Cu(2)–O(4)	2.645(3)
		Cu(2)–O(2)	1.932(2)	Cu(1)···Cu(2)	2.9631(12)
		Cu(1)···Cu(2)	3.0081(9)		
N(1)–Cu(1)–N(2)	86.2(3)	N(1)–Cu(1)–N(2)	87.60(12)	N(1)–Cu(1)–N(2)	87.90(16)
N(1)–Cu(1)–N(5)	103.7(4)	N(1)–Cu(1)–N(5)	93.25(11)	N(1)–Cu(1)–O(1)	177.48(14)
N(1)–Cu(1)–P(1)	127.2(2)	N(1)–Cu(1)–O(1)	170.39(10)	N(1)–Cu(1)–O(2)	100.18(15)
N(2)–Cu(1)–N(5)	105.5(3)	N(1)–Cu(1)–O(2)	100.65(10)	N(2)–Cu(1)–O(1)	93.20(14)
N(2)–Cu(1)–P(1)	119.1(2)	N(2)–Cu(1)–N(5)	87.74(11)	N(2)–Cu(1)–O(2)	171.35(15)
N(5)–Cu(1)–P(1)	111.3(3)	N(2)–Cu(1)–O(1)	91.77(10)	O(1)–Cu(1)–O(2)	78.61(13)
N(3)–Cu(2)–N(4)	84.5(3)	N(2)–Cu(1)–O(2)	166.59(10)	N(3)–Cu(2)–N(4)	88.73(18)
N(3)–Cu(2)–N(6)	114.9(4)	N(5)–Cu(1)–O(1)	96.31(10)	N(3)–Cu(2)–O(1)	93.28(16)
N(3)–Cu(2)–P(2)	112.3(3)	N(5)–Cu(1)–O(2)	102.18(11)	N(3)–Cu(2)–O(2)	170.79(15)
N(4)–Cu(2)–N(6)	103.6(4)	O(1)–Cu(1)–O(2)	78.32(9)	N(4)–Cu(2)–O(1)	174.69(14)
N(4)–Cu(2)–P(2)	121.4(4)	N(3)–Cu(2)–N(4)	87.31(11)	N(4)–Cu(2)–O(2)	99.08(16)
N(6)–Cu(2)–P(2)	116.3(3)	N(3)–Cu(2)–N(6)	94.41(12)	O(2)–Cu(2)–O(1)	78.52(12)
		N(3)–Cu(2)–O(1)	90.99(10)	Cu(1)–O(1)–Cu(2)	100.07(13)
		N(3)–Cu(2)–O(2)	161.14(10)	Cu(1)–O(2)–Cu(2)	102.75(15)
		N(4)–Cu(2)–N(6)	93.17(11)		
		N(4)–Cu(2)–O(1)	169.83(10)		
		N(4)–Cu(2)–O(2)	100.96(10)		
		N(6)–Cu(2)–O(1)	96.96(11)		
		N(6)–Cu(2)–O(2)	101.95(11)		
		O(1)–Cu(2)–O(2)	77.87(9)		
		Cu(1)–O(1)–Cu(2)	100.66(10)		
		Cu(1)–O(2)–Cu(2)	102.20(11)		
		N(1)–Cu(1)–N(2)	87.60(12)		

Considering all metal–ligand coordination angles, a distorted tetrahedral geometry around each copper(I) is implicated (Table 2). The Cu–NCMe bond distances[50a] are shorter than the Cu–N(amine) bond distances (Table 2).[28,50a] This shortening of Cu–NCMe bond length is expected, given the π-accepting property of MeCN. The Cu–PPh_3 bond length is the longest 2.178(3) Å, as expected.[53]

(b) $[Cu^{II}_2(L^{H,H}-O)(OH)(MeCN)_2][ClO_4]_2$ (5) and $[Cu^{II}_2(L^{Me,Me}-O)(OH)(OClO_3)][ClO_4]\cdot MeCN$ (6). Perspective views of the cationic part of **5** and **6** are displayed in Figure S19 of the Supporting Information and Figure 5, respectively. Selected bond lengths and bond angles are shown in Table 2. A MeCN molecule is present as a solvent of crystallization in the crystal of **6**. X-ray analysis revealed the incorporation of two O atoms into the complex: one into the aryl C–H bond and the other into the hydroxo bridge.

The molecular structure of the dinuclear cation in **5** reveals two five-coordinate copper(II) ions, which are bridged by a phenolate oxygen O(1) and by O(2) of a hydroxide ion. Bridging atoms occupy equatorial positions in the coordination sphere of the copper(II) ions. The equatorial coordination of each Cu^{II} center is completed by bis-methylated alkyl nitrogen donor atoms [N(1) for Cu(1) and N(4) for Cu(2)] and a secondary aliphatic amine nitrogen atom [N(2) for Cu(1) and N(3) for Cu(2)] from the terminals of the dinucleating ligand, $L^{H,H}$–O(−). The apical position of each copper(II) center is occupied by a MeCN molecule. The geometry around each copper(II) is a distorted square pyramidal [τ = 0.063 for Cu(1) and 0.145 for Cu(2)].[54] In **6**, the two copper(II) ions are essentially in a square-planar coordination environment. The

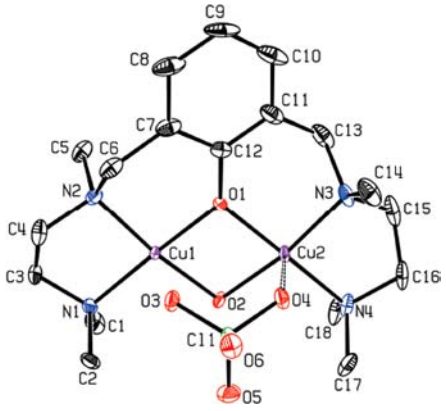

Figure 5. Perspective view of the metal coordination environment in the crystal of $[Cu^{II}_2(L^{Me,Me}-O)(OH)(OClO_3)][ClO_4]\cdot MeCN$ (**6**). Hydrogen atoms are omitted for clarity.

dx.doi.org/10.1021/ic3013848 | Inorg. Chem. 2012, 51, 13148–13161

coordination about each Cu^{II} center is completed with two amine nitrogens from the terminals of the dinucleating ligand, $L^{Me,Me}$–O(−), two oxygen atoms from the bridging phenolate O(1), and hydroxide O(2). The axial site of Cu(2) is, however, occupied by a distant oxygen atom of ClO_4^-, completing a square-pyramidal geometry around the Cu(2) center. The distance between Cu(2) and the perchlorate oxygen atom, O(4), is 2.645(3) Å, implying weak coordination.[28]

Average Cu–O(phenoxide) distance [1.9535(2) Å for **5** and 1.933(3) Å for **6**] is slightly longer than the average Cu–O(H) distance [1.9325(2) Å for **5** and 1.8965(3) Å for **6**]. For **5**, the average Cu–N (secondary aliphatic amine nitrogen) distance [1.9945(3) Å] is slightly shorter than the Cu–N(bis-methylated alkyl nitrogen) distance [2.0205(3) Å]. This trend can be explained given the steric effect associated with bis-methylated alkyl nitrogen. For **6**, the average Cu–N(amine) distance is 1.996(4) Å and the average Cu–N(bis-methylated alkyl nitrogen) distance is 2.010(4) Å. The Cu–O(Ph/H)–Cu bond angles of the phenolate or hydroxide are normal [**5**: 100.66(10)° and 102.20(11)°, respectively; **6**: 100.07(13)° and 102.75(15)°, respectively]. The Cu···Cu separations are 3.0081(9) Å for **5** and 2.9631(12) Å for **6**. The Cu(1) and Cu(2) atoms are displaced from the mean N_2O_2 plane by 0.1670 Å and 0.2222 Å, respectively, for **5** toward the apical N of MeCN. For **6**, the Cu atoms lie more or less in the plane (0.044 Å and 0.0802 Å). The mean deviations of Cu(1)N(1)-N(2)O(1)O(2) and Cu(2)N(3)N(4)O(2)O(1) with regard to the mean planes are only 0.0427 Å and 0.0754 Å, respectively, for **5** and 0.0154 Å and 0.0286 Å, respectively, for **6**. Notably, these planes make a dihedral angle of 7.684(7)° with each other in **5** and 0.773(6)° in **6**.

Magnetism. The magnetic susceptibility measurements on powdered samples of phenoxo- and hydroxo-bridged dicopper(II) complexes **5** and **6** were carried out in the temperature range of 50–300 K. The value of μ_{eff}/Cu at 300 K is found to be 0.93 μ_B for **5** and 0.97 μ_B for **6**. Overlay plots of $\chi_M T$ versus T for **5** and **6** are displayed in Figure 6. The behavior is typical of an antiferromagnetically coupled system. The data were fitted to the modified Bleany–Bowers expression (eq I)[55,56] for two interacting $S = 1/2$ centers developed under the usual isotropic (Heisenberg) exchange Hamiltonian, $\hat{H} = -JS_1S_2$.

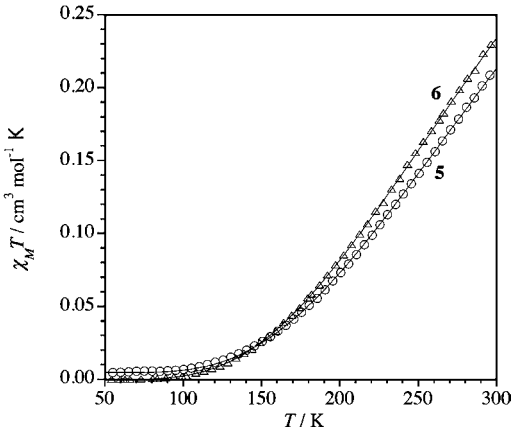

Figure 6. Plots of $\chi_M T$ versus T for powdered samples of $[Cu^{II}_2(L^{H,H}–O)(OH)(MeCN)_2][ClO_4]_2$ (**5**) and $[Cu^{II}_2(L^{Me,Me}–O)(OH)(OClO_3)][ClO_4]\cdot MeCN$ (**6**). The solid lines represent the best theoretical fit using the equations described in the text.

$$\chi_M = 2Ng^2\beta^2/3kT[1 + 1/3\exp(-J/kT)]^{-1}(1-\rho) + (Ng^2\beta^2/2kT)\rho \quad \text{(I)}$$

Inclusion of a term for possible sample contamination of a monomeric copper(II) impurity exhibiting Curie behavior yielded the appropriate equation (eq I). In this expression, N, g, β, and k have their usual meaning. χ_M is the molar susceptibility per dimer, ρ is the fraction of monomeric impurity; J corresponds to the energy difference between the singlet and triplet states. Nonlinear regression analysis was carried out with J, g, and ρ as floating parameters in the case of **5** and J and g for **6**. The best-fit parameters obtained are $J = -528$ cm^{-1}, $g = 2.09$, and $\rho = 0.01$ (1%) for **5** and $J = -505(5)$ cm^{-1} and $g = 2.11(1)$ for **6**. It is worth mentioning here that the phenoxo- and hydroxo-bridged dicopper(II) complex with $-N(Me)CH_2CH_2(2-C_5H_4N)$, in spite of the $-N(Me)-CH_2CH_2N(Me)_2$ terminal coordination as in **5** and **6**, exhibited a J value of −440 cm^{-1}.[19d]

It is worth mentioning here that for the dihydroxo-/diphenoxo-bridged dicopper(II) systems, a number of magnetostructural correlations have been attempted.[57,58] As a consequence, very useful linear correlations do exist.[58] The difference in the extent of antiferromagnetic exchange coupling between **5** and **6** could be rationalized if we consider Cu···Cu separations.

The μ_{eff}/Cu values at 300 K for **5** and **6** in MeCN solution were determined by the NMR method. At room temperature, the solution-state μ_{eff}/Cu values are 1.10 μ_B for **5** and 1.21 μ_B for **6**. Thus, the solid-state structure is retained in solution, but with a relaxed geometry.

Catechol Oxidase Activity. In this work, we have considered four phenoxo- and hydroxo-bridged dicopper(II) complexes (Figure 7) for the catechol oxidase model

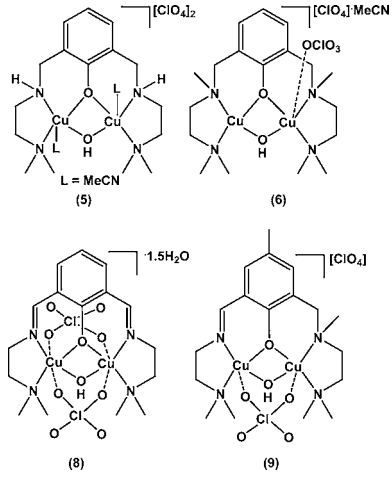

Figure 7. Schematic view of the phenoxo- and hydroxo-bridged dicopper(II) complexes considered in the catechol oxidase study.

study.[30–41] To authenticate the identity of complex **9**, ESI-MS spectrum of **9** along with its simulated spectrum is displayed in Figure S20 of the Supporting Information. Our aim is to pinpoint the effect of fine-tuning the electronic properties and stereochemical flexibility/rigidity of the dicopper(II) site on the catechol oxidase activity, as assessed by monitoring the increase in the characteristic absorption band of quinone (3,5-DTBQ) formation at 400 nm as a function of time. The formation of 3,5-DTBQ was further authenticated by ^{1}H NMR

dx.doi.org/10.1021/ic3013848 | Inorg. Chem. 2012, 51, 13148–13161

(Figure S21 of the Supporting Information). For all the complexes, saturation kinetics were found for the initial rates versus the 3,5-DTBC concentration. Representative results are displayed in Figure 8, Figure 9, and Figures S22–S24 of the

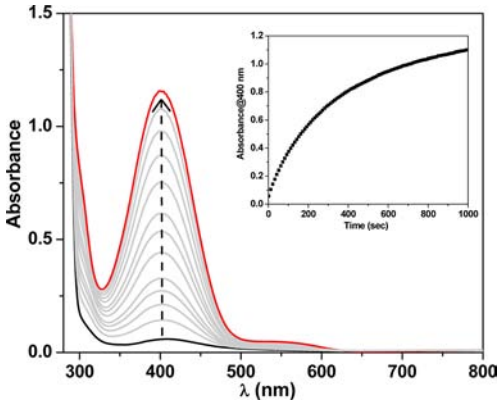

Figure 8. Formation of 3,5-DTBQ due to aerobic oxidation of 3,5-DTBC in the presence of complex **6** (Conditions: $[\mathbf{6}]_f = 2.5 \times 10^{-5}$ M and $[3,5\text{-DTBC}]_f = 1.00 \times 10^{-3}$ M in dioxygen-saturated MeOH at 303 K). Inset plot: Growth of 400 nm band over time (1000 s).

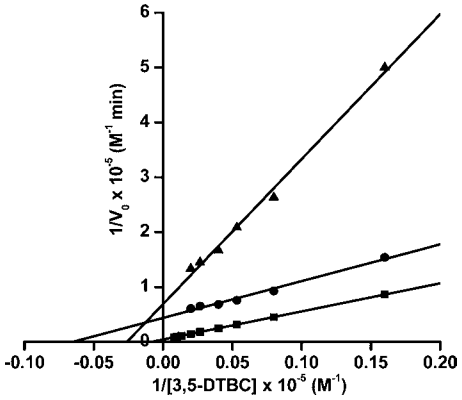

Figure 9. Lineweaver–Burk plot for aerobic oxidation of 3,5-DTBC by complexes: (●) **5**; (■) **6**; and (▲) **8**.

Table 3. Kinetic Parameters for the Oxidation of 3,5-DTBC Catalyzed by Dicopper(II) Complexes

complex	$V_{max} \times 10^6$ (M min^{-1})	K_M (mM)	$K_{ass} \times 10^{-3}$ (M^{-1})	k_{cat} (h^{-1})	$k_{cat}/K_M \times 10^{-3}$ (M^{-1} h^{-1})
5	23	0.15	6.66	55	367
6	235	1.20	0.83	564	470
8	15	0.40	2.50	36	90
9	23	0.43	2.33	55	128

Supporting Information, and in Table 3. For a fixed 3,5-DTBC concentration, the effect of variation of catalyst concentration was also investigated. In each case, a linear relationship between the initial rates and the complex concentration was obtained, indicating a first-order dependence of the rate on the catalyst concentration. A representative case for **6** is displayed in Figure S24 of the Supporting Information.

The kinetic values (Table 3) for **5**, **6**, **8**, and **9** obtained here are in accordance with our previous observation.[43] The observed k_{cat} values range from 36 to 564 h^{-1}. The best catalyst in this series (complex **6**) shows better activity than the reported ones with similar structures;[32a,33c,34b,38d] however, it shows moderate activity compared to the most efficient model catalyst reported to date ($k_{cat} = 3.24 \times 10^4$ h^{-1}).[41] Understandably, the individual factors of the ratio k_{cat}/K_M give more insight. For instance, complex **6** exhibits, by far, the largest k_{cat}, but its efficiency is limited by the large K_M value. This is likely due to the N-methyl groups on the xylyl-amine nitrogens of the ligand $L^{Me,Me}$ that probably hinder substrate association with the dicopper(II) sites of the complex, producing a 10-fold increase in K_M. Using less sterically hindered catechols than the present 3,5-DTBC may thus show a different trend in the activity of the complexes. We plan to do such studies in the near future.

The observed trend **6** > **5** > **9** > **8** (Table 3) can be rationalized based on the proposed mechanistic steps of catechol oxidase activity.[4b,36,37] It has been proposed that the reactions occur in two phases.[4b,36] The native met μ-hydroxo-dicopper(II) form reacts with one equiv of the substrate, generating the corresponding quinone and the dicopper(I) form. The latter binds dioxygen in a μ–η^2:η^2 mode, resulting in the formation of the peroxo-dicopper(II) form, which then oxidizes one more equiv of catechol to quinone with restoration of the original met form of the enzyme. Casella and co-workers demonstrated a fast initial phase followed by a slower second phase of reaction.[36] If a dicopper(II) system fails to do the second phase, only stoichiometric or very low catalytic efficiency is expected to occur. In fact, for the present complexes, only one mole of 3,5-DTBQ is formed per mole of the complex, in the absence of dioxygen. The catalytic turnover for all of the four complexes was achieved only when the experiments were conducted in the presence of dioxygen. The dioxygen is responsible for the reoxidation of the dicopper(I) form to the oxydicopper(II) form and concomitant formation of hydrogen peroxide.[59] The H_2O_2 formed could be identified by reacting with iodide to give triiodide (I_3^-).[36,37,38b,59] We have studied the formation of H_2O_2 in the course of the catalytic reaction. In fact, for all the catalytic reactions performed by the present complexes, an appreciable amount of H_2O_2 accumulation was found (Figure S25 of the Supporting Information).

The different possible catalytic cycles for oxidation of 3,5-di-*tert*-butylcatechol were summarized in Scheme 2. The H_2O_2 and 3,5-DTBQ can be generated in two possible pathways:

The difference between Path A and B is the reactivity of the oxy form, since it can react with protons or with catechol. In Path B, 3,5-DTBQ will be formed in two steps (eq 1 and 4), thereby, a biphasic reaction is expected. Depending on the rate of the reaction between these steps, either a fast initial phase and slow second phase reaction or a slow initial phase and fast second phase reaction will be expected. Casella and co-workers described a fast initial phase and slow second phase catechol oxidase activity with dinuclear copper(II) complex derived from *m*-xylyl tetrabenzimidazole ligands.[36] In contrast, the oxidation of 3,5-DTBC catalyzed by present complexes occurred in a single phase. A first-order exponential growth of 3,5-DTBQ over time (Figure 8) implies a monophasic reaction. So, we tentatively rule out Path B, assuming that the oxy form does not react with catechol to produce quinone. However, it reacts with protons to generate H_2O_2.

dx.doi.org/10.1021/ic3013848 | *Inorg. Chem.* 2012, 51, 13148–13161

Scheme 2. Different Possible Catalytic Cycle for Oxidation of 3,5-DTBC in Presence of Dicopper(II) Complexes

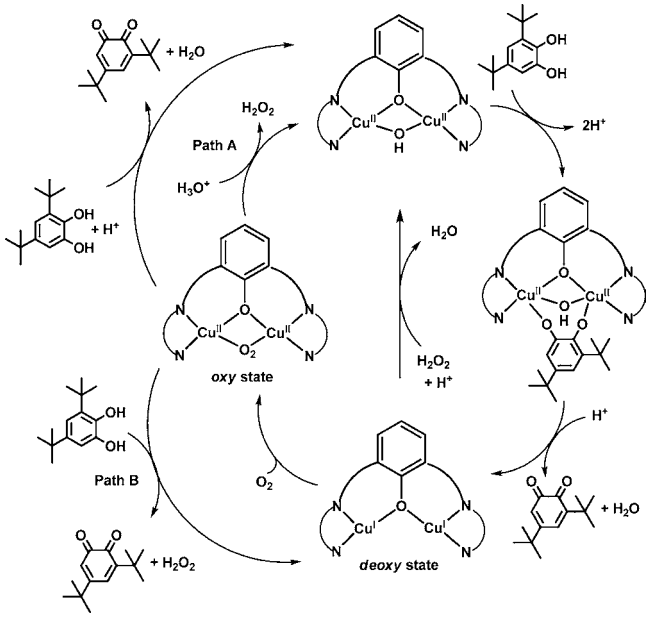

Path A:

$$Cu^{II}(OH)Cu^{II} + 3,5\text{-DTBC} \longrightarrow Cu^{I}\cdots Cu^{I} + 3,5\text{-DTBQ} + H_2O + H^+ \quad (1)$$

$$Cu^{I}\cdots Cu^{I} + O_2 \longrightarrow Cu^{II}(O_2)^{2-}Cu^{II} \quad (2)$$

$$Cu^{II}(O_2)^{2-}Cu^{II} + H_2O + H^+ \longrightarrow Cu^{II}(OH)Cu^{II} + H_2O_2 \quad (3)$$

Path B:

$$Cu^{II}(OH)Cu^{II} + 3,5\text{-DTBC} \longrightarrow Cu^{I}\cdots Cu^{I} + 3,5\text{-DTBQ} + H_2O + H^+ \quad (1)$$

$$Cu^{I}\cdots Cu^{I} + O_2 \longrightarrow Cu^{II}(O_2)^{2-}Cu^{II} \quad (2)$$

$$Cu^{II}(O_2)^{2-}Cu^{II} + 3,5\text{-DTBC} \longrightarrow Cu^{I}\cdots Cu^{I} + 3,5\text{-DTBQ} + H_2O_2 \quad (4)$$

Since the structural parameters (the Cu···Cu separation,[60] square-based geometry at the Cu^{II} center(s); the type and nature of donor atoms; and chelate-ring size) of the three complexes are similar, the differences in catalytic activity must then depend on the electronic properties of the complexes, accompanied by stereochemical flexibility modulated by the imine/amine and secondary/tertiary N atom attached to the *m*-xylyl ring. The presence of the π-accepting imine group in L^1-O^- (complex **8**) is expected to stabilize the Cu^I state more compared to $L^{H,H}-O^-$ (complex **5**) and $L^{Me,Me}-O^-$ (complex **6**). Understandably, the situation for L^2-O^- (complex **9**) is expected to be in between **8**, on one hand, and **5** and **6**, on the other. So, it is reasonable to assume that the second phase of the reaction during catecholase activity, eq 2 of Path A/Path B, would take place at a slower rate in the case of **8** compared to **5**, **6**, and **9**. This accounts for the lower catalytic efficiency (k_{cat}/K_M) of **8** compared to **5**, **6**, and **9**. However, because of the more flexible nature, the ligands $L^{H,H}-O^-$ and $L^{Me,Me}-O^-$ are better suited to facilitate initial binding of the substrate, as well as subsequent release of the product. The variation in activity between **5** and **6** may be attributed to the difference in the electron-releasing effect between the $-NCH_3-$ ($L^{Me,Me}-O^-$) and $-NH-$ ($L^{H,H}-O^-$) groups. Vittal et al. demonstrated that the presence of electron-withdrawing groups decreased the activity while electron-donating groups enhanced the activity of the complexes,[35c] justifying our contention.

It is understandable that the redox potential value of the Cu^{II}/Cu^I process should act as a predictor to the efficacy of molecular oxygen to reoxidize the reduced copper(I) centers to the copper(II) centers to bring the chemical reactions on a catalytic mode.[38b] The reduction potentials for the complexes **5**, **6**, **8**, and **9** were thus measured by cyclic voltammetry (CV) in MeCN. The data are summarized in Table 4. All four complexes show irreversible cathodic reduction peaks (Figures S26–S29 of the Supporting Information), which are tentatively assigned to processes $Cu^{II}Cu^{II} \rightarrow Cu^{II}Cu^I$ (cathodic peak potential, $E_{pc}^{(1)}$) and $Cu^{II}Cu^I \rightarrow Cu^ICu^I$ (cathodic peak potential, $E_{pc}^{(2)}$). From Table 4, it is obvious that the $2e^-$ reduced species Cu^ICu^I of **6** ($L^{Me,Me}-O^-$) is the strongest reducing agent, whereas the $2e^-$ reduced species of **8** (L^1-O^-)/**9** (L^2-O^-) [the difference in the $E_{pc}^{(2)}$ (cathodic potential for the most cathodic response) values between **8** and **9** is within experimental error] are the weakest among four complexes. So, we believe that the second phase of reaction in the catechol oxidase activity (i.e., the reaction rate of dioxygen with dicopper(I) species) will follow the order **6** > **5** > **8**/**9**. This accounts for the observed catalytic activity: **6** > **5** > **9** > **8**. Interestingly, we have found a reasonably good correlation between the $E_{pc}^{(2)}$ values and the catalytic efficiency (k_{cat}/K_M) (Figure 10). Notably, the redox potential values of

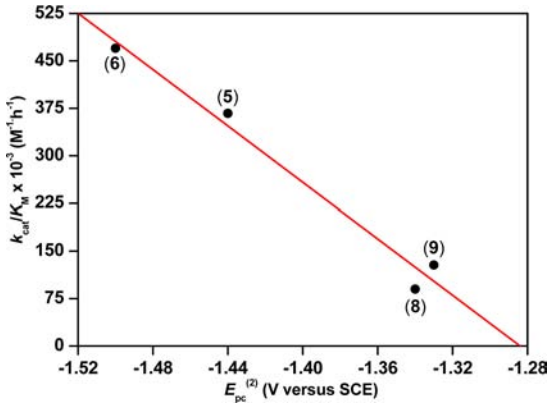

Figure 10. Correlation between $E_{pc}^{(2)}$ and catalytic efficiency (k_{cat}/K_M) for the dicopper(II) complexes **5**, **6**, **8**, and **9**.

the $Cu^{II}_2/Cu^{II}Cu^I$ and $Cu^{II}Cu^I/Cu^I_2$ couples for the present complexes are too low for an efficient catalysis (Table 4). In the case of the oxy form, the potential value(s) is expected to be

Table 4. Electrochemical Data (in MeCN) of Dicopper(II) Complexes

complex	$E_{pc}^{(1)}$ $Cu^{II,II}_2/Cu^{II,I}_2$ (V vs SCE)	$E_{pc}^{(2)}$ $Cu^{II,I}_2/Cu^{I,I}_2$ (V vs SCE)
$[Cu^{II}_2(L^{H,H}-O)(OH)(MeCN)_2][ClO_4]_2$ (**5**)	−0.85	−1.44
$[Cu^{II}_2(L^{Me,Me}-O)(OH)(OClO_3)][ClO_4]\cdot MeCN$ (**6**)	−0.64	−1.50
$[Cu^{II}_2(L^1-O)(OH)(OClO_3)_2]\cdot 1.5H_2O$ (**8**)	−0.58	−1.34
$[Cu^{II}_2(L^2-O)(OH)(OClO_3)][ClO_4]$ (**9**)	−0.55	−1.33

dx.doi.org/10.1021/ic3013848 | *Inorg. Chem.* 2012, 51, 13148–13161

even lower, as the greater σ-donating property of the peroxide group is expected to reduce the stability of the reduced state. Hence, it is expected that the oxy form will act as a poor oxidizing agent. On the other hand, it is expected that it will act as a base accepting protons, thus favoring Path A.

SUMMARY AND CONCLUDING REMARKS

In the present investigation, chemical model systems exhibiting tyrosinase-like activity and catechol oxidase-like activity have been provided. With the use of two *m*-xylyl-based dinucleating ligands, $L^{H,H}$ and $L^{Me,Me}$, providing terminal bidentate aliphatic donor nitrogens, the evidence have been obtained. Dicopper(I) complexes of $L^{H,H}$ and $L^{Me,Me}$ upon oxygenation resulted in xylyl-ring hydroxylated phenoxo- and hydroxo-bridged dicopper(II) products. A representative dicopper(I) complex, with additional PPh_3 coordination, has been structurally characterized. Structural analyses have been performed on both the xylyl-ring hydroxylated products. Reaction of the dicopper(I) complex of the ligand $L^{Me,Me}$ and dioxygen at 183 K/193 K afforded the formation of putative a bis(μ–oxo)dicopper(III) intermediate (UV–vis spectra). The low-temperature absorption spectroscopic detection of ***O*** species with the *m*-xylyl-based ligand, $L^{Me,Me}$, and decay of the putative intermediate with subsequent xylyl-ring hydroxylation is a noteworthy result. Moreover, the putative ***O*** species hydroxylates externally added phenolate as well. Thus, the results presented here are of significance in copper-dioxygen chemistry with *m*-xylyl-based ligands. In the case of $L^{Me,Me}$ during the oxygenation reaction at 298 K, an unhydroxylated dihydroxo-bridged dicopper(II) complex is also formed. Variable-temperature magnetic susceptibility measurements of phenoxo- and hydroxo-bridged complexes reveal that the two copper(II) centers, in both the complexes, are strongly antiferromagnetically coupled. The phenoxo- and hydroxo-bridged dicopper(II) complexes synthesized in this study and the two reported complexes of similar ligands have been used as models for catechol oxidase-like activity. The effect of systematic variation in the electronic properties of the dicopper(II) complexes on the catechol oxidase-like activity has been systematically investigated. In this study, it has been observed that the dicopper(II) complex derived from a flexible ligand having an electron-donating group acts as an efficient model of catechol oxidase-like activity.

ASSOCIATED CONTENT

Supporting Information

^1H and ^{13}C NMR spectra of $L^{H,H}$ and $L^{Me,Me}$ (Figures S1–S4); ^1H NMR spectra of **1**–**4** (Figures S5–S8); UV–vis spectra of **5** and **6** (Figures S9–S10); IR spectra of **6** and **7** (Figure S11); MALDI-MS spectrum of **7** (Figure S12); UV–vis spectrum (in THF) of the reaction between the dicopper(I) complex of $L^{Me,Me}$ and the dioxygen at 193 K (Figure S13); Comparative UV–vis spectra of the reaction between the dicopper(I) complex of $L^{Me,Me}$ and dioxygen in THF and in acetone at 183 K (Figure S14); UV–vis spectra of **3**·$(PF_6)_2$, bis(μ-oxo)-dicopper(III) species at 183 K, and decay product at room temperature (Figure S15); Eyring plot for thermal decay of bis(μ-oxo)dicopper(III) species of $L^{Me,Me}$ (Figure S16); UV–vis spectra of bis(μ-oxo)dicopper(III) species of $L^{Me,Me}$, after addition of 2 equiv 2,4-di-*tert*-butylphenolate, spectra after 1 h and decay profile of bis(μ-oxo)dicopper(III) species due to the reaction with 2,4-di-*tert*-butylphenolate (Figure S17); ^1H NMR spectra of the oxidation products of 2,4-di-*tert*-butylphenolate in $CDCl_3$ (Figure S18); perspective view of the metal coordination environment in the crystal of **5** (Figure S19); ESI-MS spectrum of **9** in MeCN, along with experimental and simulated mass distribution for $\{[Cu^{II}_2(L^2\text{-}O)(OH)][ClO_4]\}^+$ species (Figure S20); ^1H NMR of 3,5-DTBC and 3,5-DTBQ in $CDCl_3$ (Figure S21); dependence of the reaction rates on the 3,5-DTBC concentrations for the oxidation reaction catalyzed by **5**, **6**, and **8**. (Figure S22); Lineweaver–Burk plot for aerobic oxidation of 3,5-DTBC by **9** (Figure S23); dependence of the reaction rate on the concentration of **6** for the aerobic oxidation of 3,5-DTBC (Figure S24); electronic spectra of the formation of the I_3^- ion in the presence of H_2O_2 in the case of **5**, **6**, **8**, and **9** (Figure S25); cyclic voltammograms (Pt electrode; scan rate 100 mV/s) of **5**, **6**, **8**, and **9** in MeCN (Figures S26–S29); crystallographic data in CIF format. This material is available free of charge via the Internet at http://pubs.acs.org.

AUTHOR INFORMATION

Corresponding Author

*E-mail: rnm@iitk.ac.in, rnm@iiserkol.ac.in. Phone: +91-33-25873017. Fax: +91-33-25873028.

Present Address

[§]Indian Institute of Science Education and Research Kolkata, Mohanpur Campus, Mohanpur –741 252, India

Notes

The authors declare no competing financial interest

.

ACKNOWLEDGMENTS

This work is supported by the Department of Science & Technology (DST), Government of India, and by the Ministerio de Educación y Ciencia (MEC, Spain; Grant CTQ2007-61690 and Consolider-Ingenio in Molecular Science Grant CSD2007-00010). R.M. sincerely thanks DST for the J. C. Bose fellowship. S.M. and J.M. gratefully acknowledge the award of SRF by the Council of Scientific & Industrial Research, Government of India. We thank Prof. A. Llobet [Institute of Chemical Research of Catalonia (ICIQ), Tarragona, Spain] for use of their instrumental facilities. We thank Dr. A. De for her help in the synthesis and the catechol oxidase kinetic data of complex **9**. We also thank Mr. S. K. Barman for doing the H_2O_2 detection experiment and recording cyclic voltammograms of **5**, **6**, **8**, and **9**. S.M. thanks Mr. S. K. Barman for his help during the preparation of this manuscript. The comments of the reviewers were very helpful at the revision stage.

REFERENCES

(1) (a) Solomon, E. I.; Sundaram, U. M.; Machonkin, T. E. *Chem. Rev. (Washington, DC, U.S.)* **1996**, *96*, 2563–2605. (b) Solomon, E. I.; Chen, P.; Metz, M.; Lee, S.-K.; Palmer, A. E. *Angew. Chem., Int. Ed.* **2001**, *40*, 4570–4590. (c) Itoh, S.; Fukuzumi, S. *Acc. Chem. Res.* **2007**, *40*, 592–600.

(2) Decker, H.; Tuczek, F. *Trends Biochem. Sci.* **2000**, *25*, 392–397.

(3) (a) Matoba, Y.; Kumagai, T.; Yamamoto, A.; Yoshitsu, H.; Sugiyama, M. *J. Biol. Chem.* **2006**, *281*, 8981–8990. (b) Decker, H.; Schweikardt, T.; Tuczek, F. *Angew. Chem., Int. Ed.* **2006**, *45*, 4546–4550. (c) Rolff, M.; Schottenheim, J.; Decker, H.; Tuczek, F. *Chem. Soc. Rev.* **2011**, *40*, 4077–4098.

(4) (a) Than, R.; Feldmann, A. A.; Krebs, B. *Coord. Chem. Rev.* **1999**, *182*, 211–241. (b) Gerdemann, C.; Eicken, C.; Krebs, B. *Acc. Chem. Res.* **2002**, *35*, 183–191. (c) Selmeczi, K.; Règlier, M.; Giorgi, M.;

Speier, G. *Coord. Chem. Rev.* **2003**, *245*, 191−201. (d) Krebs, B.; Merkel, M.; Rompel, A. *J. Argentine Chem. Soc.* **2004**, *92*, 1−15. (e) Koval, I. A.; Gamez, P.; Belle, C.; Selmeczi, K.; Reedijk, J. *Chem. Soc. Rev.* **2006**, *35*, 814−840. (f) Belle, C.; Selmeczi, K.; Torelli, S.; Pierre, J.-L. *C. R. Chim.* **2007**, *10*, 271−283. (g) Ackermann, J; Buchler, S; Meyer, F. *C. R. Chim.* **2007**, *10*, 421−432.

(5) (a) Santagostini, L.; Gullotti, M.; Monzani, E.; Casella, L.; Dillinger, R.; Tuczek, F. *Chem.—Eur. J.* **2000**, *6*, 519−522. (b) Battaini, G.; De Carolis, M.; Monzani, E.; Tuczek., F.; Casella, L. *Chem. Commun.* **2003**, No. 6, 726−727. (c) Palavicini, S.; Granata, A.; Monzani, E.; Casella, L. *J. Am. Chem. Soc.* **2005**, *127*, 18031−18036. (d) Spada, A.; Palavicini, S.; Monzani, E.; Bubacco, L.; Casella, L. *Dalton Trans.* **2009**, No. 33, 6468−6471.

(6) (a) Itoh, S.; Kumei, H.; Taki, M.; Nagatomo, S.; Kitagawa, T.; Fukuzumi, S. *J. Am. Chem. Soc.* **2001**, *123*, 6708−6709. (b) Yamazaki, S.-i.; Itoh, S. *J. Am. Chem. Soc.* **2003**, *125*, 13034−13035.

(7) Citek, C.; Lyons, C. T.; Wasinger, E. C.; Stack, T. D. P. *Nat. Chem.* **2012**, *4*, 317−322.

(8) (a) Halfen, J. A.; Mahapatra, S.; Wilkinson, E. C.; Kaderli, S.; Young, V. G., Jr.; Que, L., Jr.; Zuberbühler, A. D.; Tolman, W. B. *Science* **1996**, *271*, 1397−1400. (b) Tolman, W. B. *Acc. Chem. Res.* **1997**, *30*, 227−237.

(9) Holland, P. L.; Rodgers, K. R.; Tolman, W. B. *Angew. Chem., Int. Ed.* **1999**, *38*, 1139−1142.

(10) Mirica, L. M.; Vance, M.; Rudd, D. J.; Hedman, B.; Hodgson, K. O.; Solomon, E. I.; Stack, T. D. P. *Science* **2005**, *308*, 1890−1892.

(11) Company, A; Garcia-Bosch, I.; Mas-Ballesté, R.; Que, L., Jr.; Rybak-Akimova, E.; Casella, L.; Ribas, X.; Costas, M. *Chem.—Eur. J.* **2008**, *14*, 3535−3538.

(12) Herres-Pawlis, S.; Verma, P.; Haase, R.; Kang, P.; Lyons, C. T.; Wasinger, E. C.; Flörke, U.; Henkel, G.; Stack, T. D. P. *J. Am. Chem. Soc.* **2009**, *131*, 1154−1169.

(13) Garcia-Bosch, I.; Company, A.; Frisch, J. R.; Torrent-Sucarrat, M.; Cardellach, M.; Gamba, I.; Güell, M.; Casella, L.; Que, L., Jr.; Ribas, X.; Luis, J. M.; Costas, M. *Angew. Chem., Int. Ed.* **2010**, *49*, 2406−2409.

(14) (a) Schindler, S. *Eur. J. Inorg. Chem.* **2000**, 2311−2326. (b) Tolman, W. B. *Struct. Bonding (Berlin, Ger.)* **2000**, *97*, 179−211. (c) Stack, T. D. P. *Dalton Trans.* **2003**, 1881−1889. (d) Hatcher, L. Q.; Karlin, K. *J. Biol. Inorg. Chem.* **2004**, *9*, 669−683. (e) Itoh, S.; Tachi, Y. *Dalton Trans.* **2006**, 4531−4538.

(15) (a) Mirica, L. M.; Ottenwaelder, X.; Stack, T. D. P. *Chem. Rev. (Washington, DC, U.S.)* **2004**, *104*, 1013−1045. (b) Lewis, E. A.; Tolman, W. B. *Chem. Rev. (Washington, DC, U.S.)* **2004**, *104*, 1047−1076.

(16) (a) Kitajima, N.; Fujisawa, K.; Fujimoto, C.; Moro-oka, Y.; Hashimoto, S.; Kitagawa, T.; Toriumi, K.; Tatsumi, K.; Nakamura, A. *J. Am. Chem. Soc.* **1992**, *114*, 1277−1291. (b) Kodera, M.; Katayama, K.; Tachi, Y.; Kano, K.; Hirota, S.; Fujinami, S.; Suzuki, M. *J. Am. Chem. Soc.* **1999**, *121*, 11006−11007. (c) Lam, B. M. T.; Halfen, J. A.; Young, V. G., Jr.; Hagadorn, J. R.; Holland, P. L.; Lledós, A.; Cucurull-Sánchez, L.; Novoa, J. J.; Alvarez, S.; Tolman, W. B. *Inorg. Chem.* **2000**, *39*, 4059−4072. (d) Company, A.; Lamata, D.; Poater, A.; Sola, M.; Rybak-Akimova, E. V.; Que, L., Jr.; Fontrodona, X.; Parella, T.; Llobet, A.; Costas, M. *Inorg. Chem.* **2006**, *45*, 5239−5241. (e) Company, A.; Gómez, L.; Mas-Ballesté, R.; Korendovych, I. V.; Ribas, X.; Poater, A.; Parella, T.; Fontrodona, X.; Benet-Buchholz, J.; Sola, M.; Que, L., Jr.; Rybak-Akimova, E. V.; Costas, M. *Inorg. Chem.* **2007**, *46*, 4997−5012. (f) Funahashi, Y.; Nishikawa, T.; Wasada-Tsutsui, Y.; Kajita, Y.; Yamaguchi, S.; Arii, H.; Ozawa, T.; Jitsukawa, K.; Tosha, T.; Hirota, S.; Kitagawa, T.; Masuda, H. *J. Am. Chem. Soc.* **2008**, *130*, 16444−16445.

(17) (a) Mahapatra, S.; Halfen, J. A.; Wilkin, E. C.; Pan, G.; Wang, X.; Young, V. G., Jr.; Cramer, C. J.; Que, L., Jr.; Tolman, W. B. *J. Am. Chem. Soc.* **1996**, *118*, 11555−11574. (b) Mahadevan, V.; Hou, Z.; Cole, A. P.; Root, D. E.; Lal, T. K.; Solomon, E. I.; Stack, T. D. P. *J. Am. Chem. Soc.* **1997**, *119*, 11996−11997. (c) Straub, B. F.; Rominger, F.; Hofmann, P. *Chem. Commun.* **2000**, No. 17, 1611−1612.

(18) (a) Pidcock, E.; DeBeer, S.; Obias, H. V.; Hedman, B.; Hodgson, K. O.; Karlin, K. D.; Solomon, E. I. *J. Am. Chem. Soc.* **1999**, *121*, 1870−1878. (b) Hu, Z.; George, G. N.; Gorun, S. M. *Inorg. Chem.* **2001**, *40*, 4812−4813.

(19) (a) Ghosh, D.; Lal, T. K.; Ghosh, S.; Mukherjee, R. *Chem. Commun.* **1996**, No. 1, 13−14. (b) Ghosh, D.; Lal, T. K.; Mukherjee, R. *Proceedings of the Indian Academy of Sciences (Chemical Sciences)* **1996**, *108*, 251−256. (c) Gupta, R.; Mukherjee, R. *Inorg. Chim. Acta* **1997**, *263*, 133−137. (d) Ghosh, D.; Mukherjee, R. *Inorg. Chem.* **1998**, *37*, 6597−6605. (e) Gupta, R.; Ghosh, D.; Mukherjee, R. *Proceedings of the Indian Academy of Sciences (Chemical Sciences)* **2000**, *112*, 179−186. (f) Foxon, S. P.; Utz, D.; Astner, J.; Schindler, S.; Thaler, F.; Heinemann, F. W.; Liehr, G.; Mukherjee, J.; Balamurugan, V.; Ghosh, D.; Mukherjee, R. *Dalton Trans.* **2004**, No. 15, 2321−2328.

(20) Mukherjee, R. *Proc. Indian Natl. Sci. Acad., Part A* **2004**, *70A*, 329−341.

(21) Mukherjee, R. Copper. In *Comprehensive Coordination Chemistry II: From Biology to Nanotechnology*; McCleverty, J. A.; Meyer, T. J., Eds. (Fenton, D. E., Vol. Ed.); Elsevier/Pergamon: Amsterdam, 2004; Vol. 6, pp 747−910.

(22) (a) Karlin, K. D.; Dahlstrom, P. L.; Cozzette, S. N.; Scensny, P. M.; Zubieta, J. *J. Chem. Soc., Chem. Commun.* **1981**, 881−882. (b) Karlin, K. D.; Hayes, J. C.; Gultneh, Y.; Cruise, R. W.; McKown, J. W.; Hutchinson, J. H.; Zubieta, J. *J. Am. Chem. Soc.* **1984**, *106*, 2121−2128. (c) Pidcock, E.; Obias, H. V.; Zhang, C. X.; Karlin, K. D.; Solomon, E. I. *J. Am. Chem. Soc.* **1998**, *120*, 7841−7847.

(23) Mahapatra, S.; Kaderli, S.; Llobet, A.; Neuhold, Y.-M.; Palanché, T.; Halfen, J. A.; Young, V. G., Jr.; Kaden, T. A.; Que, L., Jr.; Zuberbu1hler, A. D.; Tolman, W. B. *Inorg. Chem.* **1997**, *36*, 6343−6356.

(24) (a) Costas, M.; Ribas, X.; Poater, A.; Valbuena, J. M. L.; Xifra, R.; Company, A.; Duran, M.; Sola, M.; Llobet, A.; Corbella, M.; Usón, M. A.; Mahía, J.; Solans, X.; Shan, X.; Benet-Buchholz, J. *Inorg. Chem.* **2006**, *45*, 3569−3581. (b) Poater, A.; Ribas, X.; Llobet, A.; Cavallo, L.; Solà, M. *J. Am. Chem. Soc.* **2008**, *130*, 17710−17717.

(25) (a) Matsumoto, T.; Furutachi, H.; Kobino, M.; Tomii, M.; Nagatomo, S.; Tosha, T.; Osako, T.; Fujinami, S.; Itoh, S.; Kitagawa, T.; Suzuki, M. *J. Am. Chem. Soc.* **2006**, *128*, 3874−3875. (b) Matsumoto, T.; Furutachi, H.; Nagatomo, S.; Tosha, T.; Fujinami, S.; Kitagawa, T.; Suzuki, M. *J. Organomet. Chem.* **2007**, *692*, 111−121.

(26) Sander, O.; Henß, A.; Näther, C.; Würtele, C.; Holthausen, M. C.; Schindler, S.; Tuczek., F. *Chem.—Eur. J.* **2008**, *14*, 9714−9729 and references therein.

(27) De, A.; Mandal, S.; Mukherjee, R. *J. Inorg. Biochem.* **2008**, *102*, 1170−1189 and references therein.

(28) Mandal, S.; Mukherjee, R. *Inorg. Chim. Acta* **2006**, *359*, 4019−4026.

(29) Mandal, S.; De, A.; Mukherjee, R. *Chem. Biodiversity* **2008**, *5*, 1594−1608.

(30) Adams, H.; Fenton, D. E.; Haque, S. R.; Heath, S. L.; Ohba, M.; Okawa, H.; Spey, S. E. *J. Chem. Soc., Dalton Trans.* **2000**, 1849−1856.

(31) Complex **8** is structurally characterized but complex **9** is not, a similar complex with a saturated amine arm, $NMeCH_2CH_2NEt_2$, instead of $-NMeCH_2CH_2NMe_2$ as in **9**,[30] is structurally characterized.

(32) (a) Reim, J.; Krebs, B. *J. Chem. Soc., Dalton Trans.* **1997**, No. 20, 3793−3804. (b) Wegner, R.; Gottschaldt, M.; Görls, H.; Jäger, E.-G.; Klemm, D. *Chem.—Eur. J.* **2001**, *7*, 2143−2157.

(33) (a) Koval, I. A.; Pursche, D.; Stassen, A. F.; Gamez, P.; Krebs, B.; Reedjik, J. *Eur. J. Inorg. Chem.* **2003**, 1669−1674. (b) Koval, I. A.; Belle, C.; Selmeczi, K.; Philouze, C.; Eric, S. A.; Schuitema, A. M.; Gamez, P.; Pierre, J. L.; Reedijk, J. *J. Biol. Inorg. Chem* **2005**, *10*, 739−750. (c) Merkel, M.; Möller, N.; Piacenza, M.; Grimme, S.; Rompel, A.; Krebs, B. *Chem.—Eur. J.* **2005**, *11*, 1201−1209.

(34) (a) Torelli, S.; Belle, C.; Gautier-Luneau, I.; Pierre, J. L.; Saint-Aman, E.; Latour, J. M.; Le Pape, L.; Luneau, D. *Inorg. Chem.* **2000**, *39*, 3526−3536. (b) Torelli, S.; Belle, C.; Hamman, S.; Pierre, J.-L. *Inorg. Chem.* **2002**, *41*, 3983−3989. (c) Belle, C.; Beguin, C.; Gautier-Luneau, I.; Hamman, S.; Philouze, C.; Pierre, J. L.; Thomas, F.; Torelli, S.; Saint-Aman, E.; Bonin, M. *Inorg. Chem.* **2002**, *41*, 479−491.

(35) (a) Yang, C.-T.; Vetrichelvan, M.; Yang, X.; Moubaraki, B.; Murray, K. S.; Vittal, J. J. *Dalton Trans.* **2004**, No. 1, 113−121. (b) Sreenivasulu, B.; Vetrichelvan, M.; Zhao, F.; Gao, S.; Vittal, J. J. *Eur. J. Inorg. Chem.* **2005**, No. 22, 4635−4645. (c) Sreenivasulu, B.; Zhao, F.; Gao, S.; Vittal, J. J. *Eur. J. Inorg. Chem.* **2006**, No. 13, 2656−2670.
(36) (a) Monzani, E.; Quinti, L.; Perotti, A.; Casella, L.; Gullotti, M.; Randaccio, L.; Geremia, S.; Nardin, G.; Faleschini, P.; Tabbi, G. *Inorg. Chem.* **1998**, *37*, 553−562. (b) Monzani, E.; Battaini, G.; Perotti, A.; Casella, L.; Gullotti, M.; Santagostini, L.; Nardin, G.; Randaccio, L.; Geremia, S.; Zanello, P.; Opromolla, G. *Inorg. Chem.* **1999**, *38*, 5359−5369.
(37) Ackermann, J.; Meyer, F.; Kaifer, E.; Pritzkow, H. *Chem.—Eur. J.* **2002**, *8*, 247−258 and references therein.
(38) (a) Fernandes, C.; Neves, A.; Bortoluzzi, A. J.; Mangrich, A. S.; Rentschler, E.; Szpoganicz, B.; Schwingel, E. *Inorg. Chim. Acta* **2001**, *320*, 12−21. (b) Neves, A.; Rossi, L. M.; Bortoluzzi, A. J.; Szpoganicz, B.; Wiezbicki, C.; Schwingel, E.; Haase, W.; Ostrovsky, S. *Inorg. Chem.* **2002**, *41*, 1788−1794. (c) Peralta, R. A.; Neves, A.; Bortoluzzi, A. J.; dos Anjos, A.; Xavier, F. R.; Szpoganicz, B.; Terenzi, H.; Oliveira, M. C. B.; Castellano, E.; Friedermann, G. R.; Mangrich, A. S.; Novak, M. A. *J. Inorg. Biochem.* **2006**, *100*, 992−1004. (d) Rey, N. A.; Neves, A.; Bortoluzzi, A. J.; Pich, C. T.; Terenzi, H. *Inorg. Chem.* **2007**, *46*, 348−350.
(39) Thirumavalavan, M.; Akilan, P.; Kandaswamy, M.; Chinnakali, K.; Senthil Kumar, G.; Fun, H. K. *Inorg. Chem.* **2003**, *42*, 3308−3317.
(40) (a) Banerjee, A.; Sarkar, S.; Chopra, D.; Colacio, E.; Rajak, K. K. *Inorg. Chem.* **2008**, *47*, 4023−4031. (b) Banerjee, A.; Singh, R.; Colacio, E.; Rajak, K. K. *Eur. J. Inorg. Chem.* **2009**, No. 2, 277−284.
(41) Banu, K. S.; Chattopadhyay, T.; Banerjee, A.; Bhattacharya, S.; Suresh, E.; Nethaji, M.; Zangrando, E.; Das, D. *Inorg. Chem.* **2008**, *47*, 7083−7093.
(42) Smith, S. J.; Noble, C. J.; Palmer, R. C.; Hanson, G. R.; Schenk, G.; Gahan, L. R.; Riley, M. J. *J. Biol. Inorg. Chem.* **2008**, *13*, 499−510.
(43) Mukherjee, J.; Mukherjee, R. *Inorg. Chim. Acta* **2002**, *337*, 429−438.
(44) (a) Liang, H.-C.; Karlin, K. D.; Dyson, R.; Kaderli, S.; Jung, B.; Zuberbühler, A. D. *Inorg. Chem.* **2000**, *39*, 5884−5894. (b) Irangu, J.; Ferguson, M. J.; Jordan, R. B. *Inorg. Chem.* **2005**, *44*, 1619−1625. (c) Kubas, G. *Inorg. Synth.* **1979**, *19*, 90−92 and **1990**, *28*, 68−70.
(45) Geary, W. J. *Coord. Chem. Rev. (Washington, DC, U.S.)* **1971**, *7*, 81−122.
(46) O'Connor, C. J. *Prog. Inorg. Chem.* **1982**, *29*, 203−283.
(47) Evans, D. F. *J. Chem. Soc.* **1959**, 2003−2004.
(48) Farrugia, L. J. *WinGX version 1.64 (2003); An Integrated Systems of Windows Programs for the Solution, Refinement and Analysis of Single-Crystal X-ray Diffraction Data*, Department of Chemistry, University of Glasgow: Glasgow, Scotland, 2003.
(49) (a) Que, L., Jr.; Tolman, W. B. *Nature* **2008**, *455*, 333−340. (b) Mahadevan, V.; Klein Gebbink, R. J. M.; Stack, T. D. P. *Curr. Opin. Chem. Biol.* **2000**, *4*, 228−234. (c) Himes, R. A.; Karlin, K. D. *Curr. Opin. Chem. Biol.* **2009**, *13*, 119−131.
(50) (a) Karlin, K. D.; Haka, M. S.; Cruse, R. W.; Meyer, G. J.; Farooq, A.; Gultneh, Y.; Hayes, J. C.; Zubieta, J. *J. Am. Chem. Soc.* **1988**, *110*, 1196−1207. (b) Sanyal, I.; Murthy, N. N.; Karlin, K. D. *Inorg. Chem.* **1993**, *32*, 5330−5337.
(51) Karlin, K. D.; Nasir, M. S.; Cohen, B. I.; Cruse, R. W.; Kaderli, S.; Zuberbühler, A. D. *J. Am. Chem. Soc.* **1994**, *116*, 1324−1336.
(52) (a) However, we could not determine the accurate molar extinction coefficient values of the bis(μ-oxo)dicopper(III) species as it undergoes partial decomposition to dicopper(II) species even at 193 K. (b) Unfortunately, we cannot provide resonance Raman data due to the lack of an instrumentation facility.
(53) Taki, M.; Teramae, S.; Nagatomo, S.; Tachi, Y.; Kitagawa, T.; Itoh, S.; Fukuzumi, S. *J. Am. Chem. Soc.* **2002**, *124*, 6367−6377.
(54) Addison, A. W.; Rao, T. N.; Reedjik, J.; Van Rijn, J.; Vershcoor, G. C. *J. Chem. Soc., Dalton, Trans.* **1984**, No. 7, 1349−1356 (square-pyramidal geometry, τ = 0; trigonal-bipyramidal geometry, τ = 1).
(55) Bleaney, B.; Bowers, K. D. *Proc. R. Soc. London, Ser. A* **1952**, *214*, 451−465.
(56) Mishra, V.; Lloret, F.; Mukherjee, R. *Eur. J. Inorg. Chem.* **2007**, No. 15, 2161−2170.
(57) (a) Ruiz, E.; Alemany, P.; Alvarez, S.; Cano, J. *Inorg. Chem.* **1997**, *36*, 3683−3688. (b) Venegas-Yazigi, D.; Aravena, D.; Spodine, E.; Ruiz, E.; Alvarez, S. *Coord. Chem. Rev.* **2010**, *254*, 2086−2095.
(58) Crawford, Van H.; Richardson, H. W.; Wasson, J. R.; Hodgson, D. J.; Hatfield, W. *Inorg. Chem.* **1976**, *15*, 2107−2110.
(59) Fukuzumi, S.; Tahsini, L.; Lee, Y.-M.; Ohkubo, K.; Nam, W.; Karlin, K. D. *J. Am. Chem. Soc.* **2012**, *134*, 7025−7035.
(60) The Cu···Cu separations (Å): **5**, 3.0081(9); **6**, 2.9631(12); **8**, 2.9433(11); **9**, ∼2.96 (we assume comparable distance as that of a similar complex reported in reference 30).